Cationic Zirconium Complexes that Contain Mesityl-Substituted Diamido/Donor Ligands. Decomposition via CH Activation and Its Influence on 1-Hexene Polymerization

Yann Schrodi, Richard R. Schrock,* and Peter J. Bonitatebus, Jr.

Department of Chemistry, Massachusetts Institute of Technology, 77 Massachusetts Avenue, Cambridge, Massachusetts 02139

Received March 26, 2001

The dialkyl complexes [MesNMe]ZrMeNp (**2b**) and [MesNMe]ZrNp$_2$ ([MesNMe]$^{2-}$ = [(MesNCH$_2$CH$_2$)$_2$NMe]$^{2-}$; Np = CH$_2$CMe$_3$) were prepared and shown to have distorted trigonal bipyramidal structures in which the two amido groups occupy equatorial positions. The neopentyl group in **2b** was found in the axial position. Compound **2b** was found to convert to another species (**2a**) in a first-order manner with $k = 1.68 \times 10^{-3}$ min^{-1} at 20 °C and to reach an equilibrium with K_{eq} = [**2a**]/[**2b**] = 0.43 in C$_6$D$_6$. Activation of [MesNMe]ZrMeNp with [Ph$_3$C][B(C$_6$F$_5$)$_4$] led to formation of unobservable {[MesNMe]ZrNp}[B(C$_6$F$_5$)$_4$], which decomposed by CH activation of an ortho mesityl methyl group to give an inactive dimer of {[activ-MesNMe]Zr}[B(C$_6$F$_5$)$_4$], or in the presence of dimethylaniline by β methyl elimination to give {[MesNMe]ZrMe(PhNMe$_2$)}[B(C$_6$F$_5$)$_4$]. {[MesNMe]ZrMe}[B(C$_6$F$_5$)$_4$] also decomposes to give the dimer of {[activ-MesNMe]Zr}[B(C$_6$F$_5$)$_4$] with $k_d = 6.0 \times 10^{-5}$ s^{-1} at 20 °C. A dimethyl complex was prepared that contained a second "internal amine" donor, i.e., {[(MesNCH$_2$CH$_2$)$_2$NCH$_2$CH$_2$NMesMe]ZrMe$_2$. Upon activation of the dimethyl species with [Ph$_3$C][B(C$_6$F$_5$)$_4$], one of the (now six) ortho methyl groups was CH activated; the methyl cation was not observed. 1-Hexene was polymerized too rapidly by {[MesNMe]ZrMe}-[B(C$_6$F$_5$)$_4$] to follow readily by NMR methods, while polymerization by {[MesNMe]Zr-(PhNMe$_2$)Me}[B(C$_6$F$_5$)$_4$] and {{[MesNMe]ZrMe}$_2$(μ-Me)}[B(C$_6$F$_5$)$_4$] was found to be retarded by dimethylaniline and [MesNMe]ZrMe$_2$, respectively. The marked curvature of the log plot of the consumption of 1-hexene by {[MesNMe]Zr(PhNMe$_2$)Me}[B(C$_6$F$_5$)$_4$] could be modeled by assuming that intermediates in the polymerization process decompose by CH activation of a mesityl methyl group and are thereby removed from the system as propagating species.

Introduction

We are interested in exploring and developing diamido/donor ligands for early transition metal chemistry. One of the goals in our laboratory has been the synthesis of Zr and Hf cations that contain a diamido/donor ligand and that are active for the living polymerization of ordinary olefins, a project that began with the synthesis and study of complexes that contain the [(t-BuN-o-C$_6$H$_4$)$_2$O]$^{2-}$ ligand.[1−3] Some of the most readily accessible diamido/donor ligands that we have explored are of the type [(ArNCH$_2$CH$_2$)$_2$D]$^{2-}$, where D = O,[4,5] S,[5] or NR (R = H or Me)[6,7] and Ar is a sterically protected aryl such as 2,6-i-Pr$_2$C$_6$H$_3$ or 2,4,6-Me$_3$C$_6$H$_2$ (Mes). Ligands in which D = NMe are especially attractive in view of the greater steric protection that is exerted by the substituted central donor (versus D = O or S), the presence of only one lone electron pair on the donor, and the relative rigidity of the tridentate ligand framework.[7] The first ligand in this category that we explored was [(MesNCH$_2$CH$_2$)$_2$NMe]$^{2-}$ (or [MesNMe]$^{2-}$ in this article).[6] We showed that [MesNMe]ZrMe$_2$ can be activated with [Ph$_3$C][B(C$_6$F$_5$)$_4$] in C$_6$D$_5$Br to afford {[MesNMe]ZrMe}[B(C$_6$F$_5$)$_4$].[7] A crystal structure of a diethyl ether adduct, {[MesNMe]Zr(Et$_2$O)Me}[B(C$_6$F$_5$)$_4$], showed it to be roughly a trigonal bipyramidal species with the NMe donor and diethyl ether in apical positions. Other cations were observed, among them the dimeric monocation, {[MesNMe]$_2$Zr$_2$Me$_2$(μ-Me)}[B(C$_6$F$_5$)$_4$], which can be viewed as a [MesNMe]ZrMe$_2$ adduct of {[MesNMe]ZrMe}[B(C$_6$F$_5$)$_4$]. We found that all cations (except the diethyl etherate) would initiate the polymerization of 1-hexene and looked forward to elucidating the details of the polymerization by each type. However, we discovered that the poly-1-hexene that is produced does not have the characteristics one would expect from

(1) Baumann, R.; Davis, W. M.; Schrock, R. R. *J. Am. Chem. Soc.* **1997**, *119*, 3830.
(2) Baumann, R.; Schrock, R. R. *J. Organomet. Chem.* **1998**, *557*, 69.
(3) Schrock, R. R.; Baumann, R.; Reid, S. M.; Goodman, J. T.; Stumpf, R.; Davis, W. M. *Organometallics* **1999**, *18*, 3649.
(4) Schrock, R. R.; Schattenmann, F.; Aizenberg, M.; Davis, W. M. *Chem. Commun.* **1998**, 199.
(5) Aizenberg, M.; Turculet, L.; Davis, W. M.; Schattenmann, F.; Schrock, R. R. *Organometallics* **1998**, *17*, 4795.
(6) Liang, L.-C.; Schrock, R. R.; Davis, W. M.; McConville, D. H. *J. Am. Chem. Soc.* **1999**, *120*, 5797.
(7) Schrock, R. R.; Casado, A. L.; Goodman, J. T.; Liang, L.-C.; Bonitatebus, P. J., Jr.; Davis, W. M. *Organometallics* **2000**, *19*, 5325.

10.1021/om010247k CCC: $20.00
Publication on Web 07/10/2001

a living polymerization, and no olefinic end groups characteristic of a β hydride elimination step in the polymerization process were readily observable. We also obtained NMR evidence that {[MesNMe]Zr(PhNMe$_2$)-Me}[B(C$_6$F$_5$)$_4$] decomposed via CH bond activation of a mesityl ortho methyl group (eq 1). Therefore we began to examine the problems in systems of this type in detail. The results of this investigation are reported here. Some of these results have been reported in a preliminary communication.[8]

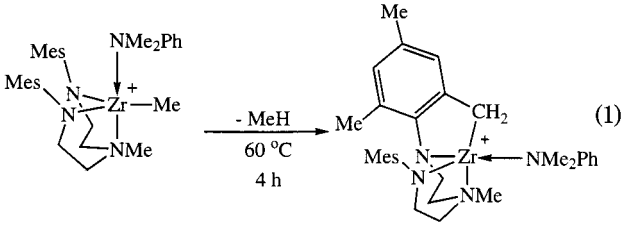

(1)

Results

Syntheses, Characterizations, and Structures of [MesNMe]ZrMeNp and [MesNMe]ZrNp$_2$ (Np = CH$_2$CMe$_3$). In view of the complications inherent in a system in which a methyl group can bridge between metal centers,[7] we sought to prepare a cation that contains an alkyl group other than methyl and one that preferably contains no β protons. We chose to prepare {[MesNMe]ZrNp}[B(C$_6$F$_5$)$_4$] (Np = CH$_2$CMe$_3$).

Addition of 1 to 2 equiv of NpMgCl to [MesNMe]ZrCl$_2$ yielded [MesNMe]ZrClNp (**1**) selectively in 90% yield (eq 2). Further alkylation of [MesNMe]ZrClNp with the

$$\text{[MesNMe]ZrCl}_2 \xrightarrow[\text{ether}]{\text{NpMgCl}} \underset{\mathbf{1}}{\text{[MesNMe]ZrClNp}} \xrightarrow[\text{ether}]{\text{MeLi}} \underset{\mathbf{2}}{\text{[MesNMe]ZrMeNp}} \quad (2)$$

neopentyl Grignard reagent is relatively slow. Complex **1** was obtained as a mixture of two isomers (**1a** and **1b**) in a 1:2 ratio, according to ^{1}H NMR spectra. Single resonances for the *tert*-butyl and methylene protons of the neopentyl group were found at 1.25 and 1.19 ppm, respectively, in **1a**, and at 0.82 and 0.62 ppm in **1b**. **1b** was isolated by recrystallization from ether at −20 °C. Treatment of pure **1b** or a mixture of **1a** and **1b** with 1 equiv of methyllithium in ether gave [MesNMe]ZrMeNp (**2**). Complex **2** was also obtained as a mixture of two isomers, **2a** and **2b**. Mixtures of **2a** and **2b** are stable in the solid state at room temperature for at least several days and for several hours in solution.

Compound **2b** could be isolated as colorless crystals from ether at −20 °C. An X-ray study (Figure 1 and Tables1 and 2) revealed **2b** to have a distorted trigonal bipyramidal structure in which the neopentyl group is located in the apical pocket opposite the NMe donor with a C(1)−Zr−N(3) angle of 166.0(4)°, and the methyl group occupies an equatorial position with a C(2)−Zr−N(3) angle of 90.7(3)°. This structure is similar to that of [t-BuNON]ZrMe$_2$ (where [t-BuNON]$^{2-}$ = [(t-BuN-o-C$_6$H$_4$)$_2$O]$^{2-}$).[1] The Zr−N$_{amido}$ bond lengths (Zr−N(1) = 2.060(6) and Zr−N(2) = 2.061(5) Å) are comparable (∼0.03 Å shorter) with those in [t-BuNON]ZrMe$_2$,[1] while

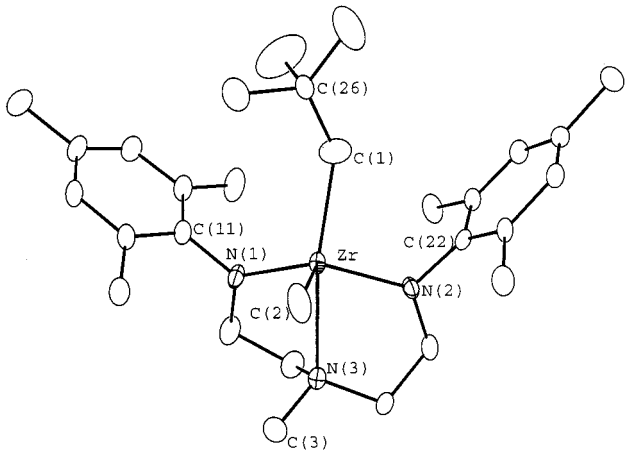

Figure 1. ORTEP drawing of the structure of [MesNMe]-ZrMeNp (**2b**).

the Zr−Me bond length (Zr−C(2) = 2.279(8) Å) is ∼0.04 Å longer than the Zr−Me$_{eq}$ bond length in [t-BuNON]-ZrMe$_2$. The Zr−N bond length to the apical donor nitrogen (Zr−N(3) = 2.488(6) Å) is slightly longer (∼0.03 Å) than in {{[MesNMe]ZrMe}$_2$(μ-Me)}[B(C$_6$F$_5$)$_4$].[7] It should be noted that the structure of **2b** is basically different from the structure of [MesNMe]ZrMe$_2$, which has the "*mer*" conformation with approximately axial amido groups in a trigonal bipyramid.[7] We believe that subtle steric factors attributable to the presence of the large neopentyl group force the structure of **2b** to be more like that of [t-BuNON]ZrMe$_2$ than that of [MesN-Me]ZrMe$_2$. Interaction of the t-Bu groups and the two methyl groups was used as an explanation as to why [t-BuNON]ZrMe$_2$ has a *fac* structure while [i-PrNON]-ZrMe$_2$ has a *mer* structure.[9]

A single crystal identical to the one used to determine the X-ray structure of **2b** was dissolved in C$_6$D$_5$Br at −15 °C. The ^{1}H NMR spectrum recorded at −15 °C revealed the presence of a minor and a major species (assumed to be **2b**) in a 5:95 ratio. Another single crystal was dissolved in C$_6$D$_6$ at room temperature, and the ^{1}H NMR spectrum obtained at 20 °C showed a similar mixture with a 10:90 ratio. In both cases the ratio of the two species changed slowly with time at room temperature and reached an equilibrium in which K_{eq} = [**2a**]/[**2b**] = 0.43 after ∼8.5 h in C$_6$D$_6$ (eq 3). The approach to equilibrium was monitored by ^{1}H NMR in C$_6$D$_6$ at 20 °C using a 29.0 mM sample, where the initial ratio [**2a**]/[**2b**] was ∼5:95. A plot of ln{([**2b**] − [**2b**]$_{eq}$)/([**2b**]$_o$ − [**2b**]$_{eq}$)} versus time is linear with a slope $k_{\mathbf{2a}} + k_{\mathbf{2b}} = 5.58 \times 10^{-3}$ min^{-1}, suggesting that the approach to equilibrium is a first-order process (Figure 2). Knowing $k_{\mathbf{2a}} + k_{\mathbf{2b}}$ and K_{eq}, we find that $k_{\mathbf{2a}} = 1.68 \times 10^{-3}$ min^{-1} and $k_{\mathbf{2b}} = 3.90 \times 10^{-3}$ min^{-1}. The process by which the two alkyl groups exchange is believed to involve either a pseudorotation pathway in the five-coordinate species or dissociation of the central nitrogen donor to give a pseudotetrahedral intermediate, followed by inversion of the free amine nitrogen and recoordination to the other CNN face in the pseudotetrahedron. We cannot assume that the structure of **2a** is also a *fac* structure analogous to **2b** in which the methyl and

(8) Schrock, R. R.; Bonitatebus, P. J., Jr.; Schrodi, Y. *Organometallics* **2001**, *20*, 1056.

(9) Baumann, R.; Stumpf, R.; Davis, W. M.; Liang, L.-C.; Schrock, R. *J. Am. Chem. Soc.* **1999**, *121*, 7822.

Table 1. Crystal Data and Structure Refinement for 2b and 3[a]

	2b	3
empirical formula	$C_{29}H_{47}N_3Zr$	$C_{33}H_{55}N_3Zr$
fw	528.93	585.04
cryst syst	orthorhombic	triclinic
space group	*P*2(1)2(1)2(1)	$P\bar{1}$
unit cell dimens	$a = 10.152(6)$ Å	10.3392(8) Å
	$b = 17.044(10)$ Å	10.7823(8) Å
	$c = 17.052(6)$ Å	15.789(1) Å
	$\alpha = 90°$	84.518(1)°
	$\beta = 90°$	76.001(1)°
	$\gamma = 90°$	77.137(1)°
volume (Å^3)	2950(3)	1663.4(2)
Z, calcd density (g/cm^3)	4, 1.191	2, 1.164
abs coeff (mm^{-1})	0.392	0.354
F(000)	1128	624
θ range for data collection (deg)	2.33 to 23.32	2.30 to 23.25
limiting indices	$-10 \le h \le 7$	$-11 \le h \le 11$
	$-18 \le k \le 10$	$-11 \le k \le 7$
	$-17 \le l \le 18$	$-17 \le l \le 17$
no. of reflns collected/unique	5661/3916	6629/4642
completeness to $\theta = 23.32$	95.7%	97.3%
max. and min. transmn	0.3264 and 0.1927	0.3693 and 0.3234
no. of data/restraints/params	3916/0/299	4642/0/380
goodness-of-fit on F^2	1.016	1.036
final *R* indices [$I > 2\sigma(I)$]	R1 = 0.0557, wR2 = 0.1300	R1 = 0.0376, wR2 = 0.1009
R indices (all data)	R1 = 0.0824, wR2 = 0.1443	R1 = 0.0416, wR2 = 0.1039
largest diff peak and hole (e·Å^{-3})	0.590 and −0.634	0.425 and −0.342

[a] All data were collected at 183(2) K using 0.71073 Å radiation and were refined by full-matrix least-squares on F^2. An empirical absorption correction was applied in each case.

Table 2. Comparison of Selected Bond Lengths (Å) and Angles (deg) in [MesNMe]ZrMeNp (2b) and [MesNMe]ZrNp$_2$ (3)

	2b	3
Zr−N(1)	2.060(6)	2.076(3)
Zr−N(2)	2.061(5)	2.086(3)
Zr−C(1)	2.256(12)	2.191(4)
Zr−C(2)	2.279(8)	2.305(3)
Zr−N(3)	2.488(6)	2.506(3)
N(1)−Zr−N(2)	123.8(2)	120.91(13)
N(1)−Zr−C(1)	110.0(5)	106.47(15)
N(1)−Zr−C(2)	111.1(3)	109.48(12)
N(1)−Zr−N(3)	71.5(2)	71.14(10)
N(2)−Zr−C(2)	109.6(3)	111.35(12)
N(2)−Zr−N(3)	71.0(2)	71.37(10)
N(2)−Zr−C(1)	97.9(3)	101.39(15)
C(1)−Zr−C(2)	101.3(6)	105.78(14)
C(1)−Zr−N(3)	166.0(4)	168.25(12)
C(2)−Zr−N(3)	90.7(3)	85.69(11)
Zr−N(1)−C(11)	124.1(5)	122.5(2)
Zr−N(2)−C(22)	120.0(4)	125.4(2)
Zr−C(1)−C(26)	143.1(7)	166.7(3)
Zr−C(2)−C(30)		132.1(2)

neopentyl groups have exchanged positions. It could be a structure of the *mer* variety, or even a structure closer to a square pyramid.

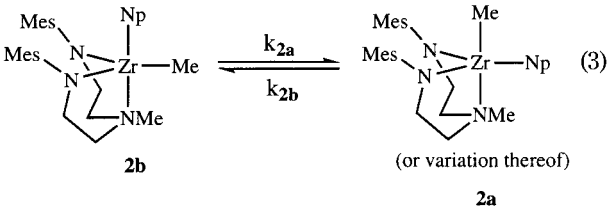

2b **2a** (3)

Proton NMR spectra of **2b** reveal the ligand's CH_2 groups as four sets of multiplets and the mesityl methyl groups as three singlets that integrate for six protons each as a consequence of restricted rotation about the C_{ipso}−N bonds. Spectra of **2a** are similar. The chemical shifts of the zirconium alkyl resonances vary considerably between **2a** and **2b**. In **2a** the *tert*-butyl, methylene, and methyl resonance shifts are 1.05, 0.91, and 0.18 ppm, respectively, whereas in **2b** they are 0.74, 0.42, and 0.55 ppm. The resonances for an alkyl in the axial position were found at higher field than those for the same alkyl in [(MesitylNSiMe$_2$CH$_2$)$_2$PPh]ZrMe$_2$, where ^{1}H NMR spectroscopy revealed resonances at −0.24 ppm for the axial methyl group and 0.88 ppm for the equatorial methyl group.[10] On this basis the relative chemical shifts for the neopentyl and methyl groups in **2a** and **2b** are consistent with the structures shown in eq 3.

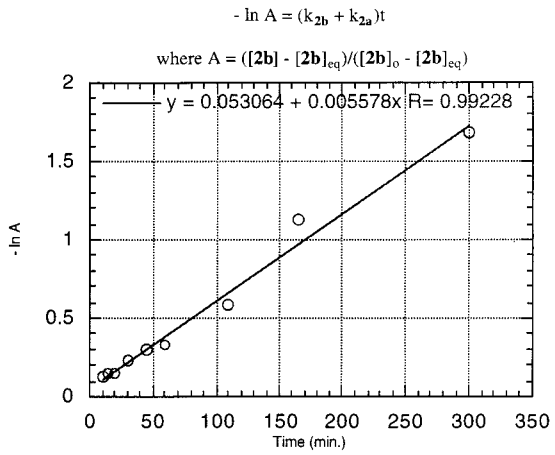

Figure 2. Approach to **2b**/**2a** equilibrium (C_6D_6; 20 °C; [**2b**]$_0$ = 29.0 mM).

[MesNMe]ZrCl$_2$ reacted with 2.3 equiv of neopentyllithium in ether to afford [MesNMe]ZrNp$_2$ (**3**) in 65% yield. Dialkylation is possible as a consequence of the higher reactivity of the lithium reagent compared to a Grignard reagent. Four singlets are found in the alkyl

(10) Schrock, R. R.; Seidel, S. W.; Schrodi, Y.; Davis, W. M. *Organometallics* **1999**, *118*, 428.

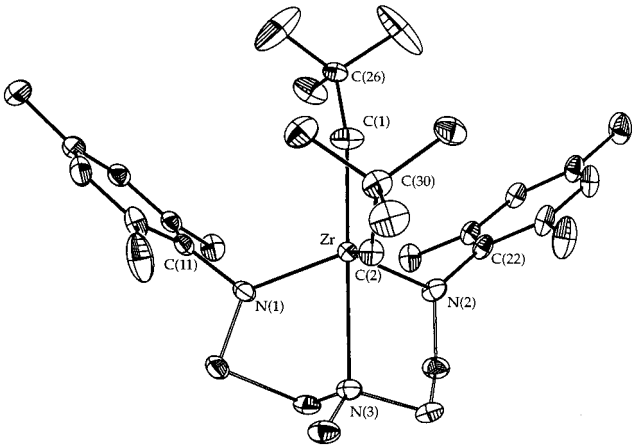

Figure 3. ORTEP drawing of the structure of [MesNMe]-$ZrNp_2$ (**3**).

region of the proton NMR spectrum of **3**, two for *tert*-butyl groups at 1.35 and 0.68 ppm and two for neopentyl methylenes at 1.15 and 0.65 ppm. We believe that the higher field resonances correspond to the axial neopentyl ligand and the lower field ones to the equatorial neopentyl ligand. The methylene carbon resonances are found at 97.5 and 82.6 ppm in a $^{13}C\{^1H\}$ NMR spectrum with $^1J_{CH} = 97$ and 104 Hz, respectively. For comparison the methylene resonance for the two equivalent $ZrCH_2$-t-Bu groups in [i-Pr-NON]$ZrNp_2$ is found at 84.6 ppm,[11] while the neopentyl methylene resonance in **2b** is found at 86.0 ppm.

Single crystals of **3** suitable for X-ray diffraction were grown from ether at −20 °C. The solid-state structure is shown in Figure 3. (See Table 2 for selected bond distances and angles.) Compound **3** has a distorted trigonal bipyramidal *fac* structure. The C(1)−Zr−N(3) angle (168.25(12)°) is comparable to that found in **2b** (166.0(4)°). In **3**, the C(2)−Zr−N(3) and C(1)−Zr−C(2) angles measure 85.69(11)° and 105.78(14)°, respectively (compared with 90.7(3)° and 101.3(6)° in **2b**), indicating that the two neopentyl groups are pushed away from each other. The Zr−C(1)−C(26) angle in the axial neopentyl group is an astonishing 166.7(3)° (compared with 143.1(7)° in **2b**), while Zr−C(2)−C(30) = 132.1(2)°. It is clear that the axial neopentyl group in **3** is under more steric pressure than the equatorial group and that the steric pressure in **3** is greater than that in **2**. An increase in the Zr−C_α−C_β angle almost certainly would lead to a reduction of the s character of the CH_2 bonds and thereby to a lower value for J_{CH}, which may help explain the slightly lower value (97 Hz) for J_{CH} in one of the neopentyl groups, presumably the axial neopentyl group. It is also interesting to note that the dihedral angle N(3)−Zr−C(2)−C(30) is close to 180° (175.0(3)°) as a consequence of steric interaction between the *tert*-butyl group containing C(30) and the methyl group attached to the central nitrogen. In effect the *tert*-butyl group that contains C(30) turns away from the NMe group, which causes the *tert*-butyl group that contains C(26) to turn away from the *tert*-butyl group that contains C(30) and encounter steric pressure from the mesityl groups. The Zr−C(1) bond length (2.191(4) Å) is much shorter (∼0.11 Å) than the Zr−C(2) bond length and is also shorter (∼0.07 Å) than the Zr−C(1) bond length in **2b**, consistent with a higher s character in the Zr−C bond of a more distorted axial neopentyl ligand. The distortion of the axial neopentyl group (and shortening of the Zr−C(1) bond) could also be accompanied by an agostic Zr−CH_α interaction,[12] although we have no independent evidence that supports that possibility. The Zr−N_{amido} bond lengths (Zr−N(1) = 2.076(3) and Zr−N(2) = 2.086(3) Å) are slightly longer than those in **2b** but somewhat shorter than those in [t-BuNON]-$ZrMe_2$.[1] The Zr−N bond length to the apical donor nitrogen (Zr−N(3) = 2.506(3) Å) is slightly longer (∼0.02 Å) than in **2b**, while the Zr−N−C_{ipso} angles (Zr−N(1)−C(11) = 122.5(2)° and Zr−N(2)−C(22) = 125.4(2)°) are similar to those found in **2b** (Zr−N(1)−C(11)° = 124.1(5) and Zr−N(2)−C(22) = 120.0(4)°).

Compound **3** slowly decomposes in C_6D_6 at room temperature over the course of several hours. We were not able to identify or isolate the products of this decomposition.

Activation of [MesNMe]$ZrNp_2$ and [MesNMe]-ZrMeNp with $[Ph_3C][B(C_6F_5)_4]$ or $[PhNHMe_2]$-$[B(C_6F_5)_4]$. The reaction between **3** and 1 equiv of $[Ph_3C][B(C_6F_5)_4]$ in C_6D_5Br proved to be very slow (relative to activation of [MesNMe]$ZrMe_2$ with $[Ph_3C]$-$[B(C_6F_5)_4]$) and relatively messy. A significant amount of **3** remained after 30 min at 0 °C. This reaction was not investigated further.

The reaction between **3** and $[PhNHMe_2][B(C_6F_5)_4]$ was also slow. More than half the starting material was left in solution after 10 min at room temperature. As the protonolysis reaction proceeded, neopentane and isobutene were formed, as well as {[MesNMe]ZrMe-$(PhNMe_2)$}$[B(C_6F_5)_4]$ and the CH activation product [(activ-MesNMe)-Zr$(PhNMe_2)$]$[B(C_6F_5)_4]$ (eq 4) in a ∼1:4 ratio. (The CH activation product was identified by ^1H NMR spectroscopy by comparison with literature data.[7]) We propose that {[MesNMe]ZrNp$(PhNMe_2)$}$[B(C_6F_5)_4]$ forms upon protonation of a neopentyl group, but it then decomposes via two different pathways, either CH activation of the ligand to give neopentane and [(activ-MesNMe)Zr$(PhNMe_2)$]$[B(C_6F_5)_4]$ (eq 4) or β Me elimination to give isobutene and {[MesNMe]ZrMe$(PhNMe_2)$}-$[B(C_6F_5)_4]$ (eq 5). (The origin of the methyl group is supported by ^{13}C labeling studies to be described later.) These results are similar to those obtained by Horton, who observed decomposition of neopentyl zirconium cations via β Me elimination to give methyl zirconium cations and isobutene.[13]

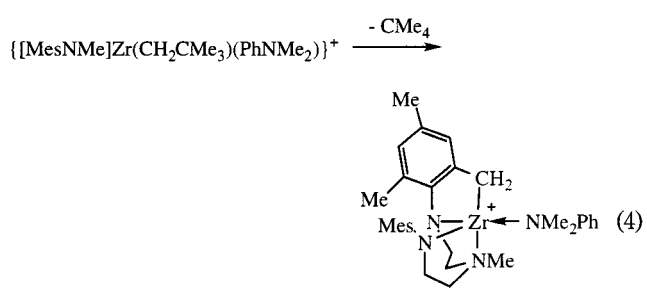

(4)

(11) Baumann, R., Ph.D. Thesis, Massachusetts Institute of Technology, 1998.

(12) Brookhart, M.; Green, M. L. H.; Wong, L. *Prog. Inorg. Chem.* **1988**, *36*, 1.

(13) Horton, A. D. *Organometallics* **1996**, *15*, 2675.

$$\{[MesNMe]Zr(CH_2CMe_3)(PhNMe_2)\}^+ \xrightarrow{-H_2C=CMe_2} \{[MesNMe]ZrMe(PhNMe_2)\}^+ \quad (5)$$

The reaction between $[Ph_3C][B(C_6F_5)_4]$ and [MesNMe]-ZrMeNp (**2**) in C_6D_5Br was much faster than that between $[Ph_3C][B(C_6F_5)_4]$ and **3**. The methyl ligand was abstracted completely and selectively at −20 °C in less than 10 min, as evidenced by complete consumption of **2** and production of Ph_3CCH_3 in high yield; no Ph_3CH, Ph_3CCH_2-t-Bu, or isobutene was formed. However, the neopentyl zirconium cation could not be observed. The presence of neopentane led us to believe that {[MesNMe]-ZrNp}$[B(C_6F_5)_4]$ had formed and decomposed via CH activation of the ligand to yield the cyclometalated product [(activ-MesNMe)Zr]$[B(C_6F_5)_4]$ (**4**) (eq 6). No significant {[MesNMe]ZrMe}$[B(C_6F_5)_4]$ was present, so CH activation of the ligand in the absence of dimethylaniline must be much faster than β Me elimination.

$$[MesNMe]ZrMeNp \xrightarrow[-Ph_3CMe]{+Ph_3C^+} \{[MesNMe]ZrNp\}^+ \xrightarrow{-CMe_4} \quad (6)$$

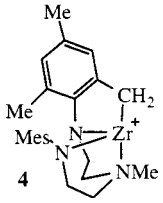

4

Dark orange crystals formed upon leaving an NMR sample of trityl-activated [MesNMe]ZrMeNp at room temperature for 2 days. X-ray diffraction showed that this species is a dimer of **4**, which we will call **4**^{2} (Figure 4, Table 3). Apparently the configuration of the ligand in **4** leaves the zirconium center exposed to binding of the arene ring, thus leading to dimerization via formation of a π complex. The coordination geometry around each zirconium center is best described as distorted square pyramidal, where the amido nitrogen atoms, the central nitrogen, and the methylene constitute the base, while the coordinated mesityl ring occupies the apical position. The N(1)−Zr(1)−N(2), N(2)−Zr(1)−N(3), and C(1)−Zr(1)−N(3) angles are similar (74.2(3)°, 70.8(2)°, and 73.9(2)°), while N(1)−Zr(1)−C(1) is much greater (98.6(3)°). The Zr−CH_2 distance Zr(1)−C(1) (2.251(7) Å) is comparable to other values observed in cationic zirconium benzyl compounds.[14] The Zr(1)−N(2) distance (2.355(7) Å) is only slightly shorter (∼0.02 Å) than the Zr−N_{donor} distance (2.373(5) Å) in $[MesNMe]ZrMe_2$, but ∼0.07 Å shorter than the Zr−N_{donor} distance (2.426(6) Å) in $\{[MesNMe]ZrMe(Et_2O)\}[B(C_6F_5)_4]$.[7] The Zr(1)−N(1) distance (2.068(7) Å) is in the range of values observed for typical Zr−N_{amido} bonds in neutral and cationic zirconium diamido-donor compounds. The other Zr−N_{amido} distance, Zr(1)−N(3) (2.190(6) Å), is ∼0.12 Å longer than Zr(1)−N(1) (2.068(7) Å). We believe that the longer Zr−N(3) bond results from relatively poor π bonding between Zr and N(3) as a consequence of the plane of the amido ligand being twisted to a significant degree from an orientation more like that found at N(1)

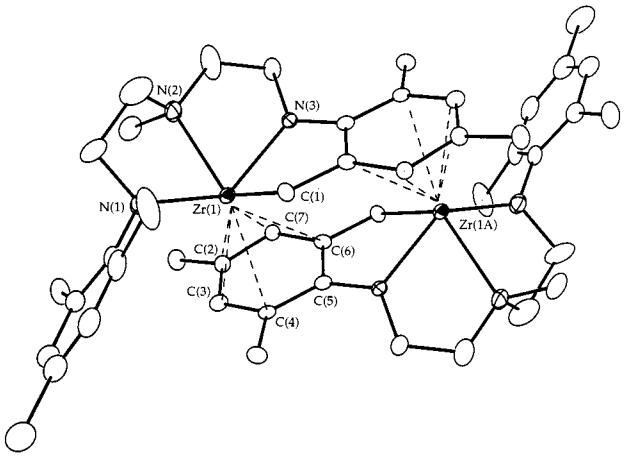

Figure 4. ORTEP drawing of the structure of the dimer of **4**.

Table 3. Selected Bond Lengths (Å) and Angles (deg) for the Dimer of 4

Bond Lengths			
Zr(1)−N(1)	2.068(7)	Zr(1)−C(3)	2.608(8)
Zr(1)−N(2)	2.355(7)	Zr(1)−C(4)	2.722(7)
Zr(1)−N(3)	2.190(6)	Zr(1)−C(6)	2.854(8)
Zr(1)−C(1)	2.251(7)	Zr(1)−C(7)	2.671(8)
Zr(1)−C(2)	2.617(7)	Zr(1)−C(5)	2.909[a]
Bond Angles			
C(1)−Zr(1)−N(2)	120.4(3)	C(1)−Zr(1)−N(3)	73.9(2)
N(1)−Zr(1)−N(2)	74.2(3)	N(1)−Zr(1)−N(3)	132.8(3)
N(1)−Zr(1)−C(1)	98.6(3)	N(2)−Zr(1)−N(3)	70.8(2)

[a] Distance according to Chem3D model.

(roughly perpendicular to the basal square plane), which we presume to be optimum for forming a Zr−N π bond. The aryl ring is not symmetrically coordinated to the zirconium atom, with the ipso carbon being further from zirconium. (Compare Zr(1)−C(5) ∼2.909 Å with the average of the remaining five carbons (∼2.69 Å).) We conclude that the Zr−arene bonding is best described as being η^5-coordinated.[14]

The dimer of **4** is highly insoluble in benzene, toluene, bromobenzene, and dimethylaniline. Reacting [MesN-Me]ZrMeNp (**2**) with 1 equiv of $[Ph_3C][B(C_6F_5)_4]$ in C_6D_5Br for 10 min followed by workup with pentane led to isolation of pure **4**^{2} according to elemental analysis (see Experimental Section) in high yield, which suggests that decomposition of the putative neopentyl zirconium cation is clean and occurs within minutes.

Observations Concerning {{[MesNMe]ZrMe}$_2$(μ-Me)}$[B(C_6F_5)_4]$ (and Other Monocationic Dimers) and Base Adducts of {[MesNMe]ZrMe}$[B(C_6F_5)_4]$. The dinuclear monocation, {{[MesNMe]ZrMe}$_2$(μ-Me)}-$[B(C_6F_5)_4]$, was initially prepared by Casado in our laboratories, and its solid-state structure was determined in an X-ray study.[7] The equatorial methyl groups in {{[MesNMe]ZrMe}$_2$(μ-Me)}$[B(C_6F_5)_4]$ were found to exchange readily between the zirconium centers on the NMR time scale, while the bridging methyl group and the equatorial methyl groups exchange relatively slowly on the NMR time scale, but still rapidly on the chemical time scale. A variety of scrambling studies confirmed this assertion. For example, addition of 1 equiv of $[MesNMe]Zr(^{13}CH_3)_2$ to {{[MesNMe]ZrMe}$_2$(μ-Me)}-$[B(C_6F_5)_4]$ in C_6D_5Br led to scrambling of the ^{13}C-labeled methyl groups in $[MesNMe]Zr(^{13}CH_3)_2$ with the unla-

(14) Pellecchia, C.; Immirzi, A.; Grassi, A.; Zambelli, A. *Organometallics* **1993**, *12*, 4473, and references therein.

beled groups in {{[MesNMe]ZrMe}$_2$(μ-Me)}[B(C_6F_5)$_4$] within a few minutes at room temperature. Therefore a [MesNMe]$ZrMe_2$ "base" must dissociate from the dimeric monocation readily on the chemical time scale. It is believed that {{[MesNMe]ZrMe}$_2$(μ-Me)}[B(C_6F_5)$_4$] can react further with trityl only because [MesNMe]-$ZrMe_2$ can dissociate and subsequently react with trityl.

An interesting question is how do [MesNMe]$ZrMe_2$ and dimethylaniline compare as bases? A 1:1 mixture of [[MesNMe]ZrMe(PhNMe_2)][B(C_6F_5)$_4$] and [MesNMe]-$ZrMe_2$ was prepared in C_6D_5Br and left at room temperature for 20 min, after which point no further change took place. The resulting mixture consisted of [[MesNMe]-ZrMe(PhNMe_2)][B(C_6F_5)$_4$], {{[MesNMe]ZrMe}$_2$(μ-Me)}-[B(C_6F_5)$_4$], [MesNMe]$ZrMe_2$, and PhNMe_2, with {{[MesN-Me]ZrMe}$_2$(μ-Me)}[B(C_6F_5)$_4$] and [[MesNMe]ZrMe-(PhNMe_2)][B(C_6F_5)$_4$] being present in a 2:1 ratio (eq 7). Therefore [MesNMe]$ZrMe_2$ turns out to be a slightly better base than dimethylaniline in a thermodynamic sense in this circumstance.

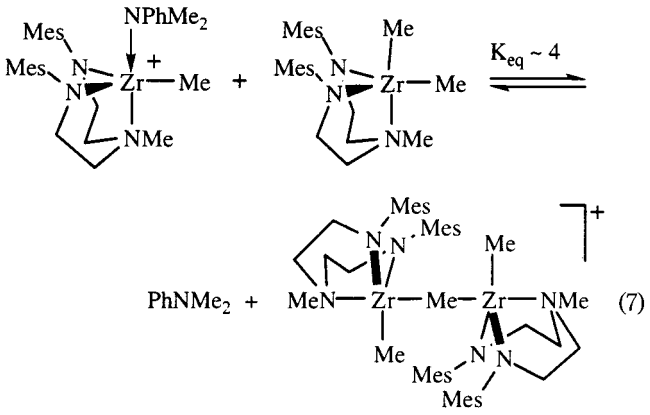

(7)

Attempts to prepare a "mixed" dinuclear species, {{[MesNMe]ZrNp}$_2$(μ-Me)}[B(C_6F_5)$_4$], by reacting [MesN-Me]ZrMeNp with 0.5 equiv of [Ph_3C][B(C_6F_5)$_4$] in C_6D_5-Br led to formation of only {{[MesNMe]ZrMe}$_2$(μ-Me)}[B(C_6F_5)$_4$], according to NMR spectroscopy. The organic byproducts were neopentane and isobutene. The same reaction performed with [MesNMe]Zr($^{13}CH_3$)Np yielded {{[MesNMe]ZrMe}$_2$(μ-Me)}[B(C_6F_5)$_4$], in which approximately 50% of the methyl groups were unlabeled, as a consequence of β Me elimination in a neopentyl ligand. The mixtures at low temperature proved too difficult to analyze readily by ^{1}H NMR spectroscopy. We believe that the "base", [MesNMe]-ZrMeNp, dissociates readily (for steric reasons) from {{[MesNMe]ZrNp}$_2$(μ-Me)}[B(C_6F_5)$_4$], and the resulting neopentyl cation decomposes via CH activation of the ligand (to give neopentane) and via β Me elimination (to give isobutene). Attempts to make the mixed dinuclear species {{[MesNMe]ZrNp}(μ-Me){[MesNMe]-ZrMe}}[B(C_6F_5)$_4$] by adding [MesNMe]ZrMeNp to {[MesNMe]ZrMe}[B(C_6F_5)$_4$] led to mixtures of species, with the major species ultimately being {{[MesNMe]-ZrMe}$_2$(μ-Me)}[B(C_6F_5)$_4$]. Addition of 1 equiv of [MesNMe]Zr($^{13}CH_3$)Np to [[MesNMe]Zr($^{13}CH_3$)][B(C_6F_5)$_4$] yielded {{[MesNMe]ZrMe}$_2$(μ-Me)}[B(C_6F_5)$_4$], which contained approximately 25% unlabeled methyl groups, again suggesting that β Me elimination competes with the CH activation in a neopentyl cation in these circumstances.

Decomposition of {[MesNMe]ZrMe}[B(C_6F_5)$_4$] and {{[MesNMe]ZrMe}$_2$(μ-Me)}[B(C_6F_5)$_4$]. The observed decomposition of {[MesNMe]ZrNp}[B(C_6F_5)$_4$] by CH activation to give **4**^{2} is not unique. {[MesNMe]ZrMe}-[B(C_6F_5)$_4$] slowly decomposes in C_6D_5Br at 20 °C to yield methane and an insoluble oil. After 2 days at room temperature, crystals suitable for X-ray diffraction crystallography were obtained in 85% yield. On the basis of a unit cell determination, these crystals were shown to be identical to **4**^{2} obtained upon decomposition of "{[N_2NMe]ZrNp}[B(C_6F_5)$_4$]". Decomposition of {[MesNMe]ZrMe}[B(C_6F_5)$_4$] was monitored by ^{1}H NMR at two different initial concentrations of {[MesNMe]-ZrMe}[B(C_6F_5)$_4$] (19.0 and 38.0 mM) in C_6D_5Br at 20 °C, using Ph_2CH_2 as an internal standard. The reactions followed strictly first-order kinetics ($R > 0.999$) with a decomposition rate constant $k_d = 6.0 \times 10^{-5}$ s^{-1}. Since "{[N_2NMe]ZrNp}[B(C_6F_5)$_4$]" cannot be observed, it must decompose more than one order of magnitude more rapidly than {[MesNMe]ZrMe}[B(C_6F_5)$_4$].

{[MesNMe]ZrMe}[B(C_6F_5)$_4$] also decomposes in a first-order manner in C_6D_5Br at 60 °C ($k_d = 2.1 \times 10^{-3}$ s^{-1} at [Zr]$_0$ = 38.0 mM), or ~16 times faster than decomposition of {[MesNMe]ZrMe(PhNMe_2)}[B(C_6F_5)$_4$] in C_6D_5Br at 60 °C ($k_d = 1.3 \times 10^{-4}$ s^{-1} at [Zr]$_0$ = 21.0 mM) to yield [(activ-MesNMe)Zr(PhNMe_2)][B(C_6F_5)$_4$].[7] Evidently dimethylaniline stabilizes the cationic methyl zirconium center toward CH activation, perhaps effectively blocking the site of a CH agostic interaction in an axial position, which likely precedes loss of alkane from an alkyl cation.

Decomposition of {{[MesNMe]ZrMe}$_2$(μ-Me)}[B(C_6F_5)$_4$] is slow at 20 °C, since [MesNMe]$ZrMe_2$ must be lost first, at least if decomposition takes place by CH activation of a mesityl methyl group. Decomposition of {{[MesNMe]ZrMe}$_2$(μ-Me)}[B(C_6F_5)$_4$] was monitored by ^{1}H NMR spectroscopy using Ph_2CH_2 as an internal standard in C_6D_5Br at 40 °C. Decomposition is strictly a first-order process with a decomposition rate constant $k_d = 9.8 \times 10^{-5}$ s^{-1} at 40 °C ($R = 0.9979$). Methane is also generated, according to ^{1}H NMR spectroscopy, as expected if decomposition takes place via dissociation of [MesNMe]$ZrMe_2$ followed by CH activation in {[MesNMe]ZrMe}[B(C_6F_5)$_4$]. However, **4**^{2} is not produced in this decomposition reaction, and we have not been able to identify the decomposition product or products. (A plausible alternative decomposition product, for example, would be a [MesNMe]$ZrMe_2$ adduct of **4**.) We cannot rule out a different mechanism for decomposition of {{[MesNMe]ZrMe}$_2$(μ-Me)}[B(C_6F_5)$_4$] or secondary decomposition of the initial decomposition product or products.

Synthesis of Complexes That Contain a Diamido/Diamine Ligand. Since coordination of a base to {[MesNMe]ZrMe}$^+$ appears to stabilize it toward decomposition via CH activation, we entertained the idea of incorporating what is approximately the equivalent of dimethylaniline connected to the central nitrogen donor, i.e., preparing species that contain a diamido/*diamine* ligand. The starting point is the known tetraamine, (MesNHCH_2CH_2)$_3$N.[15] We anticipated that selective alkylation of one of the three MesNH groups

(15) Greco, G. E.; Popa, A. I.; Schrock, R. R. *Organometallics* **1998**, *17*, 5591.

in $(MesNHCH_2CH_2)_3N$ would be difficult. Therefore we proceeded to place the tetraamine ligand on zirconium in the hope that we could in effect use the metal as a protecting group, i.e., that we could carry out chemistry on a "free" arm at some stage in the synthesis. That turned out to be the case.

Reaction of $(MesNHCH_2CH_2)_3N$ with 1 equiv of $Zr(NMe_2)_4$ gave a derivative in which one arm remains protonated and (we believe) does not coordinate to the metal (eq 8). Compound **5** is soluble in pentane but can be recrystallized at −30 °C as white crystals in 93% yield. Proton and carbon NMR spectra suggest that the mesityl rings on the amido nitrogens are equivalent and do not rotate on the NMR time scale, while the mesityl group attached to the "free arm" does rotate readily, and the dimethylamido ligands are inequivalent, consistent with the structure shown in eq 8. We believe that the reaction stops at the diamido stage for steric reasons on the basis of the fact that a similar reaction between $(4\text{-t-}BuC_6H_4NHCH_2CH_2)_3N$ and $Zr(NMe_2)_4$ led to loss of *3* equiv of dimethylamine to yield the triamidoamine derivative $[(4\text{-t-}BuC_6H_4NHCH_2CH_2)_3N]Zr(NMe_2)$.[16]

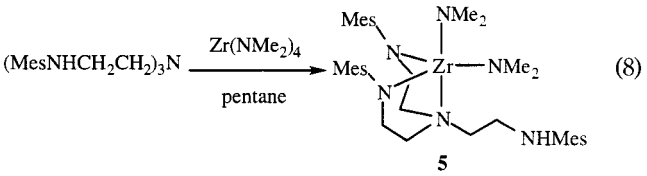

(8)

5

Addition of 1 equiv of MeLi to **5** in THF apparently led to selective deprotonation of the free NH group, on the basis of the fact that subsequent quenching with MeI gave **6a** or ^{13}C-labeled **6b** (eq 9). These reactions

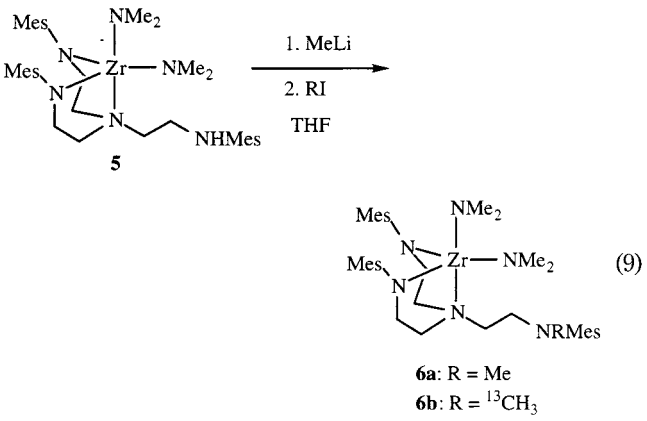

(9)

5

6a: R = Me
6b: R = $^{13}CH_3$

cannot be carried out in ether, since the product of deprotonation of **5** is insoluble in ether and for this reason reacts slowly with MeI. The NMR spectra of **6a** and **6b** are consistent with their having C_s symmetry. We believe that the third arm is not attached to the metal center for steric reasons and that inversion and rotation of the free amine is rapid on the NMR time scale. The resonances for the methyl group attached to the pendant arm in **6** are found as singlets at 2.67 and 41.79 ppm in the ^1H and $^{13}C\{^1H\}$ NMR spectra, respectively. The methyl group appears as a doublet with $^1J_{CH}$ = 134 Hz in the ^1H NMR spectrum of **6b**.

(16) Cochran, F., unpublished observations.

The reaction between **6** and 2.2 equiv of TMSCl in ether led to the facile replacement of only one dimethylamido ligand with chloride, according to ^1H NMR spectroscopy. Fortunately, the dichloride species (**7a** or **7b**) could be prepared in high yield by treating **6** with 2,6-lutidinium chloride in ether (eq 10). Subsequently, **7a** could be methylated with unlabeled or labeled methyl Grignard reagent to afford **8a** and **8c**, while **7b** could be methylated with unlabeled methyl Grignard reagent to afford **8b**, all in high yield.

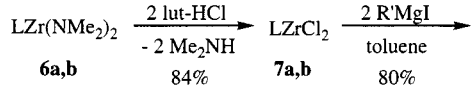

6a,b **7a,b**

L = $[(MesNCH_2CH_2)_2NCH_2CH_2NHMes]^{2-}$

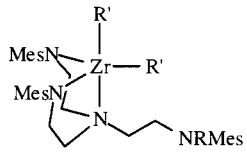

(10)

8a: R = Me, R' = Me
8b: R = $^{13}CH_3$, R' = Me
8c: R = Me, R' = $^{13}CH_3$

Compounds **7a** and **7b** are white crystalline species that are sparingly soluble in ether, benzene, and toluene. The N*Me*(Mes) resonance is found at 2.61 ppm in ^1H NMR spectra and at 41.49 ppm in $^{13}C\{^1H\}$ NMR spectra. Compounds **8** are also white crystalline species with much higher solubility in ether, benzene, and toluene than **7**. In **8** the resonances for the NMe group are found at 2.62 and 41.91 ppm in the ^1H and $^{13}C\{^1H\}$ NMR spectra, respectively. The CH coupling constant for N($^{13}CH_3$) in **7b** and **8b** is the same as it is in **6b** ($^1J_{CH}$ = 134 Hz). The resonances for the methyl ligands bound to zirconium in **8** appear at 0.28 and 0.25 ppm in ^1H NMR spectra and at 43.65 and 40.72 ppm in $^{13}C\{^1H\}$ NMR spectra. The CH coupling is the same in both methyl ligands ($^1J_{CH}$ = 114 Hz). NMR data suggest that **7** and **8** have C_s symmetry in which the two amido mesityl groups are not rotating rapidly on the NMR time scale (at room temperature) and the amino mesityl group is rotating rapidly on the NMR time scale. The free amine donor does not appear to be coordinated strongly to the metal.

Addition of 1 equiv of $[Ph_3C][B(C_6F_5)_4]$ to a colorless solution of **8c** in C_6D_5Br at −20 °C led to a bright yellow solution and evolution of gas. ^1H and $^{13}C\{^1H\}$ NMR spectroscopy revealed that $Ph_3C^{13}CH_3$, $^{13}CH_4$, and a new organometallic species, **9a**, were present in solution. According to NMR spectra, **9a** is produced quantitatively, has no symmetry, and does not contain any Zr($^{13}CH_3$) group. These results suggest that one Zr methyl group is abstracted by trityl and that the other Zr methyl group is lost as methane in a CH activation process. Reaction of **8c** with only 0.5 equiv of $[Ph_3C][B(C_6F_5)_4]$ in C_6D_5Br at −20 °C yielded a mixture of **8c** and **9a**; that is, **9a** does not interact with **8c**.

Activation of **8b** with 1 equiv of $[Ph_3C][B(C_6F_5)_4]$ in C_6D_5Br at −20 °C gave Ph_3CMe, methane, and an organometallic species, **9b**, that is identical to **9a**, except

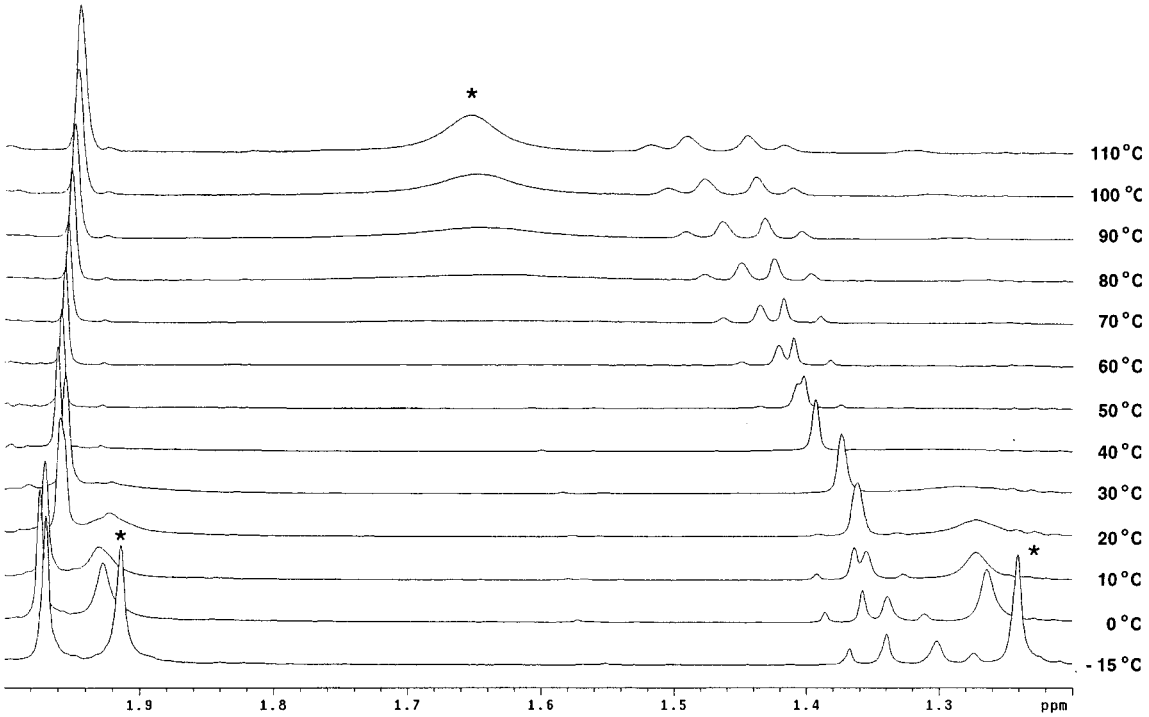

Figure 5. Variable-temperature ^{1}H NMR spectrum of **9b** in C_6D_5Br (2.0−1.2 ppm region).

a ^{13}C-labeled methyl group is attached to the amine nitrogen. It is clear that the labeled methyl group on the nitrogen donor is not activated by the cationic zirconium center. The 2.20−1.80 ppm region of the ^{1}H NMR spectrum of **9b** features one peak integrating for six protons and six single resonances integrating for three protons, one of which is broad. These resonances account for the methyl group in Ph_3CMe and for seven methyl groups attached to mesityl rings. The ^{1}H NMR spectrum of **9b** also shows an apparent AB pattern centered at 1.36 ppm ($^2J_{HH}$ = 14 Hz) that integrates as two protons, which we assign to a $ZrCH_2$ group. Finally, a broad signal at 1.27 ppm integrating for three protons may account for another methyl group attached to a mesityl ring.

Variable-temperature ^{1}H NMR spectra of **9b** between −15 and 110 °C (Figure 5) clarify matters. The two broad resonances at 1.92 and 1.27 ppm at 20 °C sharpen and shift upfield slightly when the sample is cooled and coalesce to one resonance at ∼1.65 ppm (at 110 °C) when the sample is heated. (The coalescence temperature is estimated to be ∼55 °C.) These two resonances are assigned to two ortho mesityl methyl groups. Therefore, this fluxional process can be ascribed to restricted rotation of one mesityl ring. Independent of mesityl ring rotation is an accompanying change in the AB pattern that we assign to a $ZrCH_2$ group. At −15 °C the AB pattern is located at ∼1.32 ppm, with the higher field H_B resonance being slightly broader than the resonance for H_A. As the temperature is raised to 40 °C, the chemical shifts of H_A and H_B become the same, so essentially a singlet is found for the two at ∼1.4 ppm. At higher temperatures the AB pattern re-forms as the resonance for H_B moves downfield of that for H_A.

We believe that **9a** and **9b** result from CH activation of an ortho methyl attached to one of the mesityl rings and in which the second amine donor is now bound to the metal. On the basis of NMR data, we cannot tell whether the amido mesityl or the amino mesityl ring is activated by the zirconium cationic center. However, on the basis of the formation of **4**[2] and a dimethylaniline adduct of **4** we currently believe that the amido mesityl ring is activated (eq 11). Some intramolecular dissociation of the tethered amine donor would allow for more facile rotation of the mesityl ring attached to the amine nitrogen and also would likely lead to relatively significant temperature-dependent chemical shifts if a significant amount of the four-coordinate species were present at higher temperatures. Attempts to obtain crystals of **9a** were unsuccessful. An analogous tetraphenylborate salt (**9a′**) was prepared by treating **8a** with 1 equiv of $[(\eta^5\text{-}C_5H_4Me)_2Fe][BPh_4]$ in toluene. Although **9a′** proved to be crystalline, again crystals suitable for a successful X-ray study were not obtained.

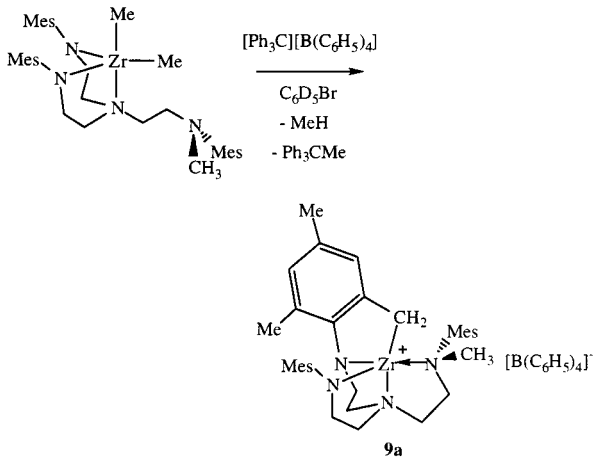

9a (11)

We conclude that the "internal base" in compounds **8** does not at all stabilize the cation obtained upon activation with trityl; that is, the hypothetical cation that would be obtained (shown in eq 12) is in fact much

less stable than {[MesNMe]ZrMe(PhNMe$_2$)}[B(C$_6$F$_5$)$_4$]. Its low stability could be ascribed to the fact that the Zr-methyl group is forced into the axial position in close proximity to an amido mesityl group, as shown in eq 12. In contrast, the dimethylaniline in {[MesNMe]ZrMe(PhNMe$_2$)}[B(C$_6$F$_5$)$_4$] is believed to be located in the apical position, as is the ether in {[MesNMe]ZrMe(Et$_2$O)}[B(C$_6$F$_5$)$_4$].[7] Therefore, CH activation and formation of **9a** is relatively rapid.

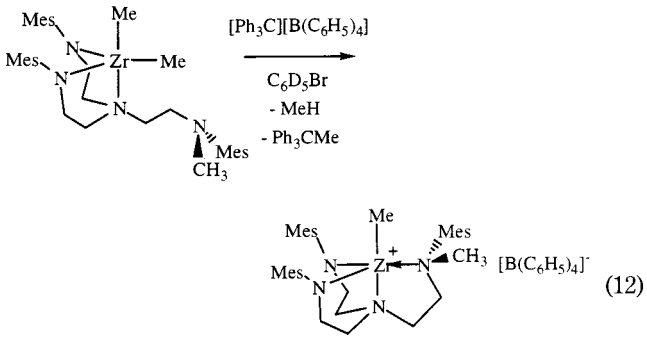

1-Hexene Polymerization Initiated by Cationic Methyl Zirconium Complexes {[MesNMe]ZrMe}[B(C$_6$F$_5$)$_4$] and {{[MesNMe]ZrMe}$_2$(μ-Me)}[B(C$_6$F$_5$)$_4$]. Polymerization reactions of 1-hexene initiated by {[MesNMe]ZrMe}[B(C$_6$F$_5$)$_4$] were too rapid to be monitored readily by ^{1}H NMR methods. Approximately 250 equiv of 1-hexene were polymerized by {[MesNMe]ZrMe}[B(C$_6$F$_5$)$_4$] at 0 °C in bromobenzene within less than 10 min at an initial metal concentration of 0.25 mM. Addition of 20 equiv of 1-hexene to a solution of {[MesNMe]ZrMe}[B(C$_6$F$_5$)$_4$] in bromobenzene at −20 °C followed by warming to 20 °C gave crystals of **4**[2] in high yield according to X-ray crystallography (unit cell match), suggesting that intermediates in this polymerization reaction also decompose by CH activation.

Polymerization of 1-hexene initiated by {{[MesNMe]ZrMe}$_2$(μ-Me)}[B(C$_6$F$_5$)$_4$] is also rapid. Approximately 150 equiv of 1-hexene were polymerized at 0 °C in bromobenzene within less than 10 min at an initial metal concentration of 0.25 mM. However, no polymerization of 1-hexene took place *even after 1 h at room temperature* when [MesNMe]ZrMe$_2$ (10 equiv) was added to the solution of {{[MesNMe]ZrMe}$_2$(μ-Me)}[B(C$_6$F$_5$)$_4$] ([cat]$_0$ = 0.25 mM). These results are consistent with competitive inhibition of polymerization by [MesNMe]ZrMe$_2$. Therefore, we propose that {{[MesNMe]ZrMe}$_2$(μ-Me)}[B(C$_6$F$_5$)$_4$] itself is not active for the polymerization of 1-hexene. Instead, {{[MesNMe]ZrMe}$_2$(μ-Me)}[B(C$_6$F$_5$)$_4$] must first dissociate into [MesNMe]ZrMe$_2$ and {[MesNMe]ZrMe}[B(C$_6$F$_5$)$_4$] in order for 1-hexene to react with {[MesNMe]ZrMe}[B(C$_6$F$_5$)$_4$]. It is likely that [MesNMe]ZrMe$_2$ can also bind to a mononuclear monocationic zirconium center that results from insertion of 1-hexene, although on the basis of the experiments described in an earlier section concerning attempted syntheses of neopentyl-containing dimeric monocations, we doubt that [MesNMe]ZrMe$_2$ binds as strongly to {[MesNMe]ZrR}[B(C$_6$F$_5$)$_4$] (where R is the growing polymer chain) as it does to {[MesNMe]ZrMe}[B(C$_6$F$_5$)$_4$]. Nevertheless, [MesNMe]ZrMe$_2$ probably binds to {[MesNMe]ZrR}[B(C$_6$F$_5$)$_4$] to some extent, and therefore a methyl group can transfer to the cationic zirconium center, as shown in eq 13. When 1-hexene is polymerized by {{[MesNMe]ZrMe}$_2$(μ-Me)}[B(C$_6$F$_5$)$_4$] in the presence of 1 equiv of [MesNMe]ZrMe$_2$ at room temperature, all [MesNMe]ZrMe$_2$ disappears as the polymerization reaction proceeds, according to ^{1}H NMR spectroscopy.

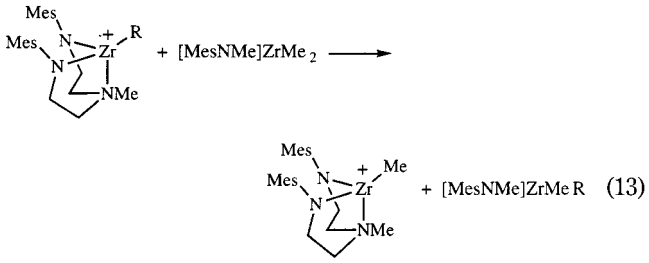

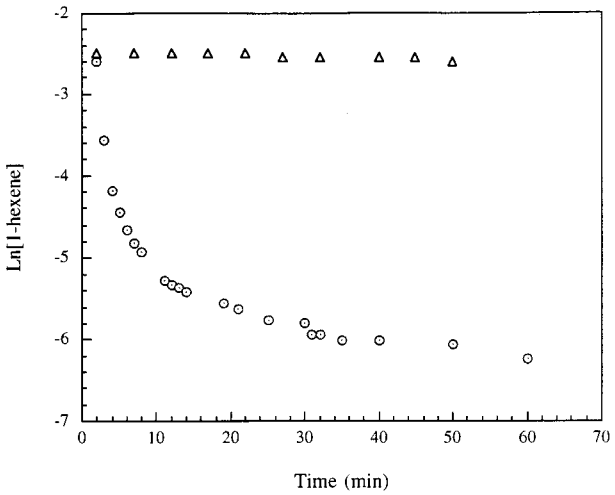

Figure 6. Kinetics of 1-hexene polymerization initiated by {{[MesNMe]ZrMe}$_2$(μ-Me)}[B(C$_6$F$_5$)$_4$] ([cat]$_0$ = 0.25 mM; 300 equiv 1-hexene; 20 °C) in the presence of 1 equiv of [MesNMe]ZrMe$_2$ (circles) and 10 equiv of [MesNMe]ZrMe$_2$ (triangles).

The consumption of 1-hexene during polymerizations initiated by {{[MesNMe]ZrMe}$_2$(μ-Me)}[B(C$_6$F$_5$)$_4$] in bromobenzene at room temperature in the presence of 1 and 10 equiv of [MesNMe]ZrMe$_2$ is shown in Figure 6. When only 1 equiv of [MesNMe]ZrMe$_2$ is present in solution, polymerization of 1-hexene proceeds at room temperature, but the plot of ln[1-hexene] vs time shows considerable curvature. Since we know that **4**[2] is formed during polymerization using {[MesNMe]ZrMe}[B(C$_6$F$_5$)$_4$] alone as the initiator, we propose that {[MesNMe]ZrR}[B(C$_6$F$_5$)$_4$] (where R is the growing polymer chain), like {[MesNMe]ZrNp}[B(C$_6$F$_5$)$_4$], decomposes readily during the polymerization reaction, in addition to reacting with [MesNMe]ZrMe$_2$ to yield [MesNMe]ZrRMe. Of course [MesNMe]ZrRMe could be activated again by loss of a methyl group and the resulting {[MesNMe]ZrR}[B(C$_6$F$_5$)$_4$] could further react with 1-hexene, etc. Methyl group transfer from a neutral Zr to a cationic Zr center is a complicating feature of the polymerization that we would like to avoid. For this reason, and since we have shown that dimethylaniline and [MesNMe]ZrMe$_2$ are approximately equally good bases toward {[MesNMe]ZrMe}[B(C$_6$F$_5$)$_4$], we turned to an exploration of polymerization of 1-hexene by {[MesNMe]ZrMe(PhNMe$_2$)}[B(C$_6$F$_5$)$_4$].

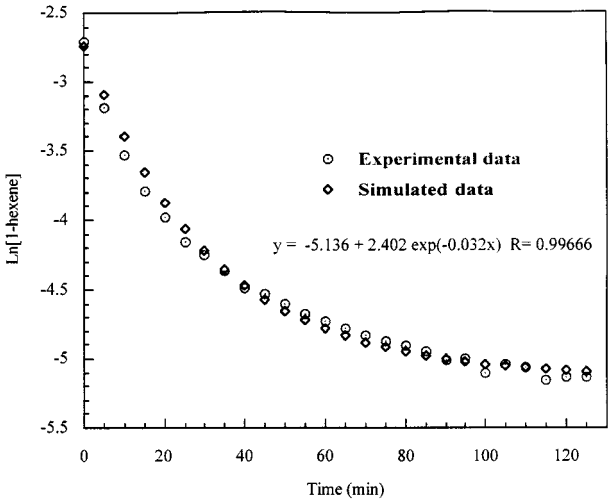

Figure 7. Kinetics of 1-hexene polymerization initiated by {[MesNMe]ZrMe(PhNMe$_2$)}[B(C$_6$F$_5$)$_4$] ([cat]$_0$ = 0.25 mM; 300 equiv 1-hexene; 0 °C). Experimental data (circles) and simulated data using eq 5 (squares).

Study of 1-Hexene Polymerization Reaction Initiated by {[MesNMe]ZrMe(PhNMe$_2$)}[B(C$_6$F$_5$)$_4$]. Addition of 300 equiv of 1-hexene to {[MesN$_2$NMe]ZrMe(PhNMe$_2$)}[B(C$_6$F$_5$)$_4$] (0.25 mM, 0 °C, C$_6$D$_5$Br) led to the formation of poly-[1-hexene] over a period of 2 h (>95% consumption of the 1-hexene). A plot of ln[1-hexene] vs time shows significant curvature (Figure 7), suggesting that the observed rate constant decreases as the reaction proceeds. Since we have observed clean first-order consumption of 1-hexene in three other diamido/donor systems in our laboratories at this stage,[8,17,18] it is clear that catalyst decomposition competes with polymerization. If this deactivation corresponds to a CH activation in a mesityl ortho methyl group at a rate that is first order in Zr and zero order in 1-hexene, and if the resulting species is inactive, then consumption of 1-hexene would obey eq 14, where k_d is the first-order rate of decomposition of the catalyst. Integration of eq 14 yields eq 15, where the constant of integration is (k_p/k_d)[cat]$_0$ + ln[1-hexene]$_0$.

$$\frac{\text{d[1-hexene]}}{\text{d}t} = -k_p[\text{cat}]_0 e^{-k_d t}[\text{1-hexene}] \quad (14)$$

$$\ln[\text{1-hexene}] = \frac{k_p}{k_d}[\text{cat}]_0 e^{-k_d t} + \text{constant} \quad (15)$$

If we fit the experimental data to eq 14, we obtain the rate constant for the first-order and irreversible decomposition of the intermediates at 0 °C, $k_d = 5.0 \times 10^{-4}$ s^{-1}. We can also obtain the observed rate constant of polymerization ($k_{obs} = 1.2 \times 10^{-3}$ s^{-1}) and therefore calculate the rate constant for the propagation of the poly-1-hexene chain, $k_p = 4.8$ M^{-1} s^{-1}, assuming that the rate of polymerization depends to the first order on 1-hexene concentration. It should be recalled that the rate constant for decomposition of {[MesNMe]ZrMe}[B(C$_6$F$_5$)$_4$] at 20 °C was found to be 6.0×10^{-5} s^{-1} and that the rate constant for decomposition of {[MesNMe]ZrNp}[B(C$_6$F$_5$)$_4$] was perhaps 1 to 2 orders of magnitude larger, or approximately 6.0×10^{-3} s^{-1} to 6.0×10^{-4} s^{-1} at 20 °C. At 0 °C these numbers would be smaller by approximately a factor of 2 for every 10°, or ~10^{-3} to 10^{-4}. Therefore an observed rate constant $k_d = 5.0 \times 10^{-4}$ s^{-1} for the first-order irreversible decomposition of polymerization intermediates at 0 °C is roughly the same as the rate constant for decomposition of {[MesNMe]ZrNp}[B(C$_6$F$_5$)$_4$]. We stress that our interpretation of the data in Figure 7 is not a unique solution to the problem, and the numbers obtained therefore need to be corroborated through other experiments.

Discussion

A central theme of this work is that {[MesNMe]ZrMe}[B(C$_6$F$_5$)$_4$] in bromobenzene is the species responsible for the polymerization of 1-hexene and that dimethylaniline and [MesNMe]ZrMe$_2$ bind competitively to {[MesNMe]ZrMe}[B(C$_6$F$_5$)$_4$] and thereby reduce the rate of polymerization. Of course the anion and/or bromobenzene are also associated with the cation to a degree that is unknown at this stage. In any case, the anion and/or bromobenzene are clearly not associated as strongly with the cation as is dimethylaniline or [MesNMe]ZrMe$_2$. As one might expect, {[MesNMe]ZrMe(Et$_2$O)}[B(C$_6$F$_5$)$_4$] is virtually inactive for polymerization of 1-hexene at room temperature, and the anion is well-separated from the cation in the solid state. Therefore there now seems little possibility that 1-hexene could react readily with any nonlabile base adduct of {[MesNMe]ZrMe}[B(C$_6$F$_5$)$_4$] via a six-coordinate intermediate. The structures of [MesNMe]ZrMeNp and [MesNMe]ZrNp$_2$ make it clear that five-coordinate species themselves are quite crowded. It should be noted that the degree to which the anion is associated with the cation in {[MesNMe]ZrMe}[B(C$_6$F$_5$)$_4$] in bromobenzene is not known.

It is also clear that activation of a CH bond in a mesityl ortho methyl group in a variety of {[MesNMe]ZrR}[B(C$_6$F$_5$)$_4$] complexes competes with polymerization of 1-hexene. However, it is curious that CH activation when R = Me is so much slower than when R = neopentyl or the growing polymer chain. It seems possible that a larger alkyl group keeps the anion further away from the zirconium cationic center, thereby allowing the mesityl ortho-methyl CH bond to interact more readily with the zirconium center and intramolecular CH bond activation to be faster. However, we should entertain the possibility that at least one of the species observed in low-temperature spectra of {[MesNMe]ZrMe}[B(C$_6$F$_5$)$_4$] is a dimeric dication, namely, {[MesNMe]ZrMe}$_2$[B(C$_6$F$_5$)$_4$]$_2$,[7] and that therefore some as yet poorly defined "dimer" of {[MesNMe]ZrMe}[B(C$_6$F$_5$)$_4$] ion pairs could stabilize the methyl cation to a significant degree toward CH activation. Higher "aggregates" of ion pairs should also be considered.[19] "Aggregates" of any size would be less likely with any {[MesNMe]ZrR}[B(C$_6$F$_5$)$_4$] species in which R is not methyl, and therefore such species should be more unstable with respect to CH activation of the mesityl's methyl group, as well as more active toward insertion of 1-hexene into the Zr−R bond.

(17) Goodman, J. T., unpublished observations.
(18) Mehrkhodavandi, P., unpublished observations.
(19) Beck, S.; Lieber, S.; Schaper, F.; Geyer, A.; Brintzinger, H.-H. *J. Am. Chem. Soc.* **2001**, *123*, 1483.

We do not believe that the process of CH activation differs in any significant way from the large number of "σ bond metatheses" in the literature.[20−24] In our case, we propose that the reaction involves activation of the mesityl ortho-methyl CH bond by the zirconium methyl group (eq 16). An interesting question is whether the mesityl methyl group can actually "displace" L from the coordination sphere, i.e., be CH activated via a six-coordinate transition state. This subtlety is difficult to answer at this stage; it would seem logical that if L is "weakly coordinated", e.g., the anion, then "displacement" would be a viable mechanistic gray area and the rate possibly quite sensitive to the size of R, as we have found.

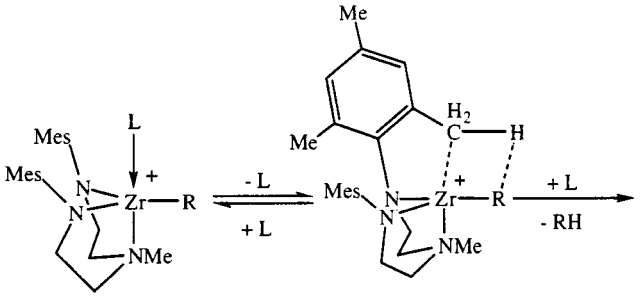

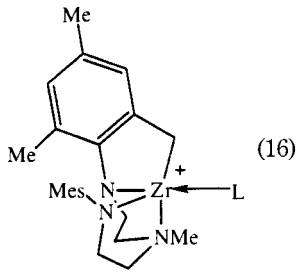

(16)

4

Decomposition of cationic Zr-methyl or Zr-benzyl complexes by loss of RH has been observed previously in several systems. Horton and co-workers reported the slow decomposition in solution of the cationic diamido-donor zirconium complex {[(TMSNCH$_2$CH$_2$)$_2$NTMS]-ZrCH$_2$Ph}[PhCH$_2$B(C$_6$F$_5$)$_3$] by CH bond activation of one of the amido TMS methyl groups and formation of toluene.[25] They proposed that the product of CH activation is a cyclometalated zirconium cation stabilized by coordination of the benzylborate anion to the zirconium atom. Marks and co-workers, upon reacting [η^5-1,3-t-Bu$_2$C$_5$H$_3$]$_2$ZrMe$_2$ with B(C$_6$F$_5$)$_3$, observed formation of a ring-metalated metallacyclic complex, resulting from intramolecular CH activation of {[η^5-1,3-t-Bu$_2$C$_5$H$_3$]$_2$-ZrMe}[MeB(C$_6$F$_5$)$_3$].[20] The reaction is quantitative and complete in less than 1 h at room temperature and generates 1 equiv of methane, according to ^{1}H NMR spectroscopy. A third example was published by Erker and co-workers, who obtained results similar to those reported by Marks upon activating [η^5-C$_5$H$_4$CMe$_2$NMe$_2$]$_2$-ZrMe$_2$ with B(C$_6$F$_5$)$_3$.[21]

Dinuclear monocations are no longer rare. For example, Horton and co-workers have observed and isolated a dinuclear monocation as an intermediate in the formation of a methyl mononuclear monocationic zirconium complex containing similar diamido-amine ligands,[25] and several examples of metallocene [Zr(μ-Me)Zr]$^+$ species are known.[26−31] Nevertheless, the finding that [MesNMe]ZrMe$_2$ is a better base than dimethyl aniline was surprising to us.

Elimination of a β methyl group from an alkyl ligand in a cationic alkyl complex is now known for a variety of transition metals.[32−37] In zirconium systems in which propylene is polymerized, elimination of a β methyl group has been recognized through identification of vinyl end groups.[38−40] Perhaps the most relevant results are those by Horton,[13] who showed that cationic zirconocene neopentyl complexes decomposed by β methyl elimination and that the process was slowed dramatically when a base such as acetonitrile was coordinated to the metal. We expect to find more examples of β methyl group elimination in diamido/donor ligand systems in due course.

Some clarification is in order at this stage concerning three polymerization reactions in our laboratory that we now know to be living for 1-hexene. The first system is the original {[(t-BuN-o-C$_6$H$_4$)$_2$O]ZrMe}[B(C$_6$F$_5$)$_4$] system, which is living up to 10 °C in chlorobenzene or bromobenzene.[17] In this case the *tert*-butyl groups on the amido nitrogens are crucial to success to the extent that they provide an especially crowded coordination sphere and therefore enforce a pseudotetrahedral arrangement about the cationic metal center. Isopropyl or aryl groups do not yield living polymerization catalysts as a consequence of competing β hydride elimination in the now more "open" and flexible coordination sphere.[7,9] In cationic [t-BuNON]$^{2-}$ complexes, CH activation processes are not fast even in the absence of 1-hexene, at least up to 10 °C. Because of the finely

(20) Yang, X.; Stern, C. L.; Marks, T. J. *J. Am. Chem. Soc.* **1994**, *116*, 10015.
(21) Bertuleit, A.; Fritze, C.; Erker, G.; Fröhlich, R. *Organometallics* **1997**, *16*, 2891.
(22) Thompson, M.; Baxter, S.; Bulls, A.; Burger, B.; Nolan, M.; Santarsiero, B.; Schaefer, W.; Bercaw, J. *J. Am. Chem. Soc.* **1987**, *109*, 203.
(23) Jordan, R. F.; Taylor, D. F.; Baenziger, N. C. *Organometallics* **1990**, *9*, 1546.
(24) Ryabov, A. D. *Chem. Rev.* **1990**, *90*, 403, and references therein.
(25) Horton, A. D.; de With, J.; van der Linden, A. J.; van de Weg, H. *Organometallics* **1996**, *15*, 2672.
(26) Beck, S.; Prosenc, M. H.; Brintzinger, H. H.; Goretzki, R.; Herfert, N.; Fink, G. *J. Mol. Catal. A* **1996**, *111*, 67.
(27) Bochmann, M.; Lancaster, S. J. *Angew. Chem., Int. Ed. Engl.* **1994**, *33*, 1634.
(28) Bochmann, M.; Lancaster, S. J.; Hursthouse, M. B.; Malik, K. M. A. *Organometallics* **1994**, *13*, 2235.
(29) Chen, Y.-X.; Stern, C. L.; Yang, S.; Marks, T. J. *J. Am. Chem. Soc.* **1996**, *118*, 12451.
(30) Jia, L.; Yang, X.; Stern, C. L.; Marks, T. J. *Organometallics* **1997**, *16*, 842.
(31) Köhler, K.; Piers, W. E.; Jarvis, A. P.; Xin, S.; Feng, Y.; Bravakis, A. M.; Collins, S.; Clegg, W.; Yap, G. P. A.; Marder, T. B. *Organometallics* **1998**, *17*, 3557.
(32) Kondo, T.; Mitsudo, T. *J. Synth. Org. Chem. Jpn.* **1999**, *57*, 552−558.
(33) McNeill, K.; Andersen, R. A.; Bergman, R. G. *J. Am. Chem. Soc.* **1997**, *119*, 11244−11254.
(34) Etienne, M.; Mathieu, R.; Donnadieu, B. *J. Am. Chem. Soc.* **1997**, *119*, 3218−3228.
(35) Dzwiniel, T. L.; Etkin, N.; Stryker, J. M. *J. Am. Chem. Soc.* **1999**, *121*, 10640−10641.
(36) Lefebvre, F.; Thivolle-Cazat, J.; Dufaud, V.; Niccolai, G. P.; Basset, J. M. *Appl. Catal. A* **1999**, *182*, 1−8.
(37) Older, C. M.; Stryker, J. M. *J. Am. Chem. Soc.* **2000**, *122*, 2784−2797.
(38) Resconi, L.; Piemontesi, F.; Franciscono, G.; Abis, L.; Fiorani, T. *J. Am. Chem. Soc.* **1992**, *114*, 1025−1032.
(39) Eshuis, J. J. W.; Tan, Y. Y.; Meetsma, A.; Teuben, J. H.; Renkema, J.; Evens, G. G. *Organometallics* **1992**, *11*, 362.
(40) Weng, W. Q.; Markel, E. J.; Dekmezian, A. H. *Macromol. Rapid Commun.* **2000**, *21*, 1103−1107.

balanced nature of the {[(t-BuN-o-C_6H_4)$_2$O]ZrMe}-[B(C_6F_5)$_4$] system, alteration of the ligand has met with limited success, at least in terms of maintaining a living polymerization.[17]

The second successful ligand system is a dimesityl diamido-amine ligand analogous to the trimethylsilyl-substituted version introduced by Gade,[41] namely, [(MesNCH_2)$_2$C(Me)(2-C_6H_4N)]$^{2-}$ (or [MesNpy]$^{2-}$ here). The {[MesNpy]ZrMe}[B(C_6F_5)$_4$] system is much more "open" as a consequence of the diamido/donor being less flexible and held back more rigidly in a strictly *fac* manner.[42] In this case formation of a monocationic dinuclear species [(Mes_2N_2Npy)$_2$$Zr_2Me_3$][B($C_6F_5$)$_4$] is a serious limitation since the dinuclear species does not lose [MesNpy]ZrMe_2 readily and therefore does not react readily with additional [Ph_3C][B(C_6F_5)$_4$]. This limitation can be overcome through the use of larger alkyl groups such as isobutyl in the initiator. Even though β hydride elimination in {[MesNpy]Zr(isobutyl)}[B(C_6F_5)$_4$] takes place slowly at 0 °C, the reaction with 1-hexene is relatively fast and no β hydride elimination takes place after polymerization has begun. Most importantly, CH activation in the mesityl group in this system does *not* seem to be a limitation in any cation we have explored so far. We have shown recently that analogous Hf systems are strictly living by establishing the stability of a variety of {[MesNpy]HfR}[B(C_6F_5)$_4$] species at 0 °C along with a high reactivity toward insertion of 1-hexene.[18] In species of this type the mesityl groups adopt a more "open" bowl-like arrangement so that even when they rotate so as to aim the ortho methyl group toward the metal, the metal is beyond reach for the presumably required agostic CH interaction.

The third successful ligand system, the [(2,6-$Cl_2C_6H_3$-NCH_2CH_2)$_2$NMe]$^{2-}$ ligand,[8] arose from the simple fact that bromobenzene and chlorobenzene are compatible solvents in polymerizations of the type we have been discussing. Although the ortho chlorides interact with the metal to some degree in {[(2,6-$Cl_2C_6H_3$NCH_2CH_2)$_2$-NMe]ZrR}$^+$ species, that interaction does not result in deactivation. These catalysts, and the as yet unprepared Hf analogues, show significant promise in terms of further elucidating the variety of constructive and destructive processes taking place at the cationic Zr center.

Conclusions

We have shown that {[(MesNCH_2CH_2)$_2$NMe]ZrMe}-[B(C_6F_5)$_4$] and related "base adducts" are initiators for the polymerization of 1-hexene and that intermediates in the polymerization reaction especially are highly susceptible to CH activation in a mesityl ortho methyl group to give what appears to be an inactive species, at least in the relatively insoluble dimeric form that is found in the solid state. Any living character of 1-hexene polymerization in this system therefore is severely compromised. Since zirconium or hafnium complexes that contain the [(MesNCH_2)$_2$C(Me)(2-C_6H_4N)]$^{2-}$ ligand do not suffer from CH activation, mesityl CH activation will not necessarily be widespread and in some cases can be avoided altogether, e.g., by employing 2,6-$Cl_2C_6H_3$ aryl groups on the amido nitrogens.

Experimental Section

General Procedures. All experiments were performed under a nitrogen atmosphere in a Vacuum Atmospheres drybox or by standard Schlenk techniques unless specified otherwise. Tetrahydrofuran and diethyl ether were sparged with nitrogen and passed through two columns of activated alumina. Toluene was distilled from sodium/benzophenone ketyl. Pentane was sparged with nitrogen and passed through one column of activated alumina and then through another column of activated Q5. Chlorobenzene (Aldrich HPLC Grade, 99.9%) was distilled from CaH_2 under nitrogen. All solvents were stored in the drybox over 4 Å molecular sieves. 1-Hexene was refluxed over sodium for 4 days, distilled, and stored over 4 Å sieves. Molecular sieves and Celite were activated in vacuo (10^{-3} Torr) for 24 h at 175 and 125 °C, respectively.

Reported NMR chemical shifts are listed as parts per million downfield from tetramethylsilane. Routine coupling constants are not reported. Spectra were obtained in C_6D_6 at 22 °C unless otherwise noted. Elemental analyses were performed by H. Kolbe Microanalytical Laboratory, Mülheim an der Ruhr, Germany.

Zr(NMe_2)$_4$,[43] [MesNMe]ZrCl_2,[7] and [MesNMe]ZrMe_2[7] were prepared according to the literature procedures, and [Ph_3C]-[B(C_6F_5)$_4$] was provided by Exxon Chemical Corporation. All other chemicals were purchased from commercial suppliers and used as received.

[MesNMe]ZrClNp (1). A 0.9 M solution of NpMgCl in ether (2.5 mL, 2.25 mmol) was added via syringe to a chilled slurry of [MesNMe]ZrCl_2 (1.02 g, 2.0 mmol) in toluene (30 mL). The reaction mixture was stirred for 2 h and then treated with an excess of dioxane. The off-white precipitate was filtered off on a bed of Celite, and the solvents were removed under reduced pressure. The solid residue was washed with pentane (2 × 10 mL) and dried under reduced pressure to afford a coral powder (1.0 g, 1.8 mmol) in 90% yield. ^{1}H NMR revealed that the product was obtained as a mixture of two isomers (**1a** and **1b**) in a 1:2 ratio. **1a**: ^{1}H NMR δ 6.93 (s, 2, Ar), 6.91 (s, 2, Ar), 3.30 (m, 2, CH_2), 3.10 (m, 2, CH_2), 2.57 (s, 6, Me_o), 2.57 (m, 2, CH_2), 2.46 (s, 6, Me_o), 2.18 (m, 2, CH_2), 2.15 (s, 6, Me_p), 2.13 (s, 3, NMe), 1.25 (s, 9, ZrCH_2C(CH_3)$_3$), 1.19 (s, 2, ZrCH_2C-(CH_3)$_3$). **1b**: ^{1}H NMR δ 6.91 (s, 4, Ar), 3.42 (m, 2, CH_2), 2.98 (m, 2, CH_2), 2.65 (s, 6, Me_o), 2.58 (m, 2, CH_2), 2.40 (s, 6, Me_o), 2.20 (s, 3, NMe), 2.18 (m, 2, CH_2), 2.14 (s, 6, Me_p), 0.82 (s, 9, ZrCH_2C(CH_3)$_3$), 0.62 (s, 2, ZrCH_2C(CH_3)$_3$). **1b** was isolated by crystallization from ether. Anal. Calcd for $C_{28}H_{44}N_3ClZr$: C, 61.22; H, 8.07; N; 7.65; Cl: 6.45. Found: C, 61.31; H, 8.06; N, 7.72; Cl: 6.34.

[MesNMe]ZrMeNp (2). A 1.4 M solution of MeLi in ether (1.2 mL, 1.68 mmol) was added via syringe to a chilled solution of [MesNMe]ZrClNp (0.90 g, 1.64 mmol) in ether (20 mL). The reaction mixture was stirred for 30 min and filtered through Celite, and the solvents were removed under reduced pressure to afford a solid that is a mixture of two isomers (**2a** and **2b**) in a 1:5 ratio according to ^{1}H NMR spectroscopy. Recrystallization from ether/pentane at −20 °C gave **2b** (0.60 g, 1.13 mmol) in 69% yield: ^{1}H NMR δ 6.97 (s, 2, Ar), 6.94 (s, 2, Ar), 3.36 (m, 2, CH_2), 3.18 (m, 2, CH_2), 2.63 (s, 6, Me_o), 2.55 (m, 2, CH_2), 2.40 (s, 6, Me_o), 2.19 (s, 6, Me_p), 2.17 (m, 2, CH_2), 2.07 (s, 3, NMe), 0.74 (s, 9, ZrCH_2C(CH_3)$_3$), 0.55 (s, 3, ZrMe), 0.42 (s, 2, ZrCH_2C(CH_3)$_3$); ^{13}C NMR δ 147.66 (C, Ar), 135.44 (C, Ar), 135.01 (C, Ar), 134.53 (C, Ar), 130.46 (CH, Ar), 130.11 (CH, Ar), 85.96 (ZrCH_2C(CH_3)$_3$), 57.60 (CH_2), 55.61 (CH_2), 43.81 (ZrMe), 40.48 (NMe), 35.51 (ZrCH_2C(CH_3)$_3$), 34.86 (ZrCH_2C(CH_3)$_3$), 21.52 (Me_p), 19.80 (Me_o), 19.54 (Me_o). Anal. Calcd for $C_{29}H_{47}N_3Zr$: C, 65.85; H, 8.96; N; 7.94. Found: C, 66.04; H, 9.10; N, 7.85.

(41) Friedrich, S.; Schubart, M.; Gade, L. H.; Scowen, I. J.; Edwards, A. J.; McPartlin, M. *Chem. Ber. Rec.* **1997**, *130*, 1751.

(42) Mehrkhodavandi, P.; Bonitatebus, P. J., Jr.; Schrock, R. R. *J. Am. Chem. Soc.* **2000**, *122*, 7841.

(43) Diamond, G. M.; Jordan, R. F.; Petersen, J. L. *Organometallics* **1996**, *15*, 4030.

[MesNMe]ZrNp$_2$ (3). A solution of NpLi (71 mg, 0.92 mmol) in ether (2 mL) was cooled at −20 °C for 10 min and added to a cold slurry of [MesNMe]ZrCl$_2$ (205 mg, 0.4 mmol) in ether (5 mL). The reaction mixture was warmed to room temperature and stirred for 15 min. The white precipitate was filtered off on a Celite bed, and the volatile solvents were removed from the filtrate under reduced pressure. The residual solid was washed with pentane (2 × 2 mL) and dried under reduced pressure to afford a yellow solid material (150 mg, 0.26 mmol) in 65% yield: ^{1}H NMR δ 6.93 (s, 4, Ar), 3.33 (m, 2, CH$_2$), 3.12 (m, 2, CH$_2$), 2.63 (m, 2, CH$_2$), 2.60 (s, 6, Me$_o$), 2.48 (s, 6, Me$_o$), 2.21 (m, 2, CH$_2$), 2.19 (s, 3, NMe), 2.18 (s, 6, Me$_p$), 1.35 (s, 9, ZrCH$_2$C(C*H*$_3$)$_3$), 1.15 (s, 2, ZrC*H*$_2$C(CH$_3$)$_3$), 0.68 (s, 9, ZrCH$_2$C(C*H*$_3$)$_3$), 0.65 (s, 2, ZrC*H*$_2$C(CH$_3$)$_3$); ^{13}C NMR δ 149.27 (C, Ar), 134.86 (C, Ar), 134.72 (C, Ar), 134.16 (C, Ar), 130.36 (CH, Ar), 130.17 (CH, Ar), 97.45 (Zr*C*H$_2$C(CH$_3$)$_3$), 82.63 (Zr*C*H$_2$C(CH$_3$)$_3$), 56.87 (CH$_2$), 55.53 (CH$_2$), 36.75, 36.17, 36.06, 34.52, 21.31, 20.05.

Dimer of [(activ-MesNMe)Zr][B(C$_6$F$_5$)$_4$] (4^2). [Ph$_3$C][B(C$_6$F$_5$)$_4$] (76 mg, 0.08 mmol) was added as a solid to a cold solution (−30 °C) of **2** (42 mg, 0.08 mmol) in C$_6$H$_5$Br (2 mL). The solution immediately turned dark orange, and evolution of gas was observed. The solution was stirred for 10 min at room temperature and was then added to vigorously stirred cold pentane (4 mL). An orange solid precipitated and was collected on a frit. The solid was washed with more pentane (2 × 2 mL) and dried under reduced pressure to give an orange powder that was not soluble in C$_6$D$_5$Br; yield ∼80%. Anal. Calcd for C$_{47}$H$_{32}$N$_3$BF$_{20}$Zr: C, 50.37; H, 2.88; N; 3.75. Found: C, 50.46; H, 2.85; N, 3.68.

Single Crystals of 4^2. [Ph$_3$C][B(C$_6$F$_5$)$_4$] (88.0 mg, 94.5 μmol) was added to a cold solution (−30 °C) of [MesNMe]ZrMe$_2$ (45.0 mg, 94.5 μmol) in C$_6$D$_5$Br (2.0 mL) in a 4 mL vial to yield {[MesNMe]ZrMe}[B(C$_6$F$_5$)$_4$] quantitatively according to the ^{1}H NMR spectrum. The orange solution was then left at room temperature for 2 days to give dark orange needles of **4^2** (105.0 mg, 80.3 μmol) in 85% yield (after decanting C$_6$D$_5$Br, washing with pentane, and drying in vacuo). The crystals were insoluble in benzene, toluene, bromobenzene, *N*,*N*′-dimethylaniline, or a mixture of bromobenzene and *N*,*N*′-dimethylaniline.

[(MesNCH$_2$CH$_2$)$_2$NCH$_2$CH$_2$NHMes]Zr(NMe$_2$)$_2$ (5). Zr(NMe$_2$)$_4$ (1.02 g, 3.8 mmol) was added as a solid to a solution of (MesNHCH$_2$CH$_2$)$_3$N (1.91 g, 3.8 mmol) in toluene (20 mL) that had been previously cooled to −20 °C. The reaction mixture was stirred at room temperature for 5 h. The volatile solvents were then removed under reduced pressure. Pentane (20 mL) was added to the residual oil, and the solution was allowed to stand at −30 °C overnight. The pentane was decanted and the crystalline material was collected and dried under reduced pressure to afford a white solid (2.4 g, 3.5 mmol) in 93% yield: ^{1}H NMR δ 6.93 (s, 4, Ar), 6.79 (s, 2, Ar), 3.39 (m, 2, CH$_2$), 3.12 (m, 4, CH$_2$), 3.07 (s, 6, NMe$_2$), 2.93 (m, 4, CH$_2$), 2.66 (m, 2, CH$_2$), 2.49 (s, 6, Me$_{Ar}$), 2.43 (s, 6, Me$_{Ar}$), 2.36 (s, 6, NMe$_2$), 2.19 (s, 6, Me$_{Ar}$), 2.19 (s, 6, Me$_{Ar}$), 2.17 (s, 3, Me$_{Ar}$); ^{13}C{^{1}H} NMR δ 150.03, 143.17, 134.43, 133.99, 132.24, 130.44, 130.34, 129.72, 129.63, 53.75 (s, CH$_2$), 52.58 (s, CH$_2$), 44.94 (s, NMe$_2$), 42.68 (s, NMe$_2$), 41.49 (s, CH$_2$), 21.41 (s, Me), 21.23 (s, Me), 19.96 (s, Me), 19.62 (s, Me), 19.06 (s, Me). Anal. Calcd for C$_{37}$H$_{58}$N$_6$Zr: C, 65.53; H, 8.62; N, 12.39. Found: C, 65.48; H, 8.70; N, 12.23.

[(MesNCH$_2$CH$_2$)$_2$NCH$_2$CH$_2$N(Me)Mes]Zr(NMe$_2$)$_2$ (6a). A 1.4 M solution of MeLi in ether (1.59 mL, 2.2 mmol) was added dropwise to a solution of **5** (1.43 g, 2.1 mmol) in THF (35 mL) that had been cooled to −20 °C. Gas evolution was observed as MeLi was added and proceeded for a couple of minutes after addition was complete. The reaction mixture turned yellow and was stirred at room temperature for 5 min after gas evolution ceased. An excess of MeI (270 μL) was then added via syringe at room temperature. The solution turned colorless immediately and slowly became cloudy. The reaction mixture was left at room temperature for 35 min. The volatile components were removed under reduced pressure, and ether (30 mL) was added to the residue. A white solid was filtered off on Celite and washed with ether (2 × 5 mL). The volume of the solution was reduced to ∼15 mL in vacuo, and some solid material precipitated. The vial was stored at −20 °C overnight, and the crystalline material was collected on a frit, washed with pentane (2 × 5 mL), and dried in vacuo to afford a white powder (1.59 g), which contains approximately one molecule of THF per Zr, according to ^{1}H NMR spectroscopy; yield 94%. The THF adduct can be used as is or recrystallized slowly from ether at −20 °C over a fews days to afford a THF free product: ^{1}H NMR δ 6.94 (s, 4, Ar), 6.80 (s, 2, Ar), 3.39 (m, 2, CH$_2$), 3.10 (m, 6, CH$_2$), 3.06 (s, 6, NMe$_2$), 2.85 (m, 2, CH$_2$), 2.67 (s, 3, NMe), 2.62 (m, 2, CH$_2$), 2.50 (s, 6, Me$_{Ar}$), 2.44 (s, 6, Me$_{Ar}$), 2.37 (s, 6, NMe$_2$), 2.29 (s, 6, Me$_{Ar}$), 2.19 (s, 6, Me$_{Ar}$), 2.15 (s, 3, Me$_{Ar}$); ^{13}C{^{1}H} NMR δ 150.10, 145.96, 137.62, 135.61, 134.42, 134.02, 132.21, 130.49, 129.73, 129.61, 53.77 (s, CH$_2$), 52.30 (s, CH$_2$), 51.01 (s, CH$_2$), 47.98 (s, CH$_2$), 44.79 (s, NMe$_2$), 42.72 (s, NMe$_2$), 41.79 (s, NCH$_3$), 21.34 (s, Me), 21.24 (s, Me), 19.91 (s, Me), 19.62 (s, Me), 19.55 (s, Me). Anal. Calcd for C$_{38}$H$_{60}$N$_6$Zr: C, 65.94; H, 8.74; N, 12.14. Found: C, 66.12; H, 8.80; N, 12.06.

[(MesNCH$_2$CH$_2$)$_2$NCH$_2$CH$_2$N(^{13}CH$_3$)Mes]Zr(NMe$_2$)$_2$ (6b). The ^{13}C-labeled analogue of **6a** was prepared in a manner similar to that for **5** using ^{13}CH$_3$I as the alkylating agent. NMR data are analogous to those for **6a** except the resonance for the labeled methyl in the ^{1}H NMR spectrum appears as a doublet at 2.67 ppm ($^1J_{CH}$ = 134 Hz).

[(MesNCH$_2$CH$_2$)$_2$NCH$_2$CH$_2$N(Me)Mes]ZrCl$_2$ (7a). Two equivalents of lutidinium chloride (220 mg, 1.53 mmol) was added as a solid to a solution of **6a** (530 mg, 0.766 mmol) in ether (30 mL) at −20 °C. A white solid precipitated rapidly from solution. The white precipitate was collected on a frit, washed with pentane (2 × 5 mL), and dried to afford white crystalline product (435 mg, 0.645 mmol) in 84% yield: ^{1}H NMR δ 6.88 (s, 2, Ar), 6.81 (s, 2, Ar), 6.78 (s, 2 Ar), 3.44 (m, 4, CH$_2$), 2.98 (m, 4, CH$_2$), 2.78 (m, 2, CH$_2$), 2.62 (m, 2, CH$_2$), 2.61 (s, 3, NMe), 2.48 (s, 6, Me$_{Ar}$), 2.45 (s, 6, Me$_{Ar}$), 2.26 (s, 6, Me$_{Ar}$), 2.12 (s, 9, Me$_{Ar}$). Anal. Calcd for C$_{34}$H$_{48}$Cl$_2$N$_4$Zr: C, 60.51; H, 7.17; N, 8.30; Cl, 10.51. Found: C, 60.68; H, 7.23; N, 6.98; Cl, 10.59.

[(MesNCH$_2$CH$_2$)$_2$NCH$_2$CH$_2$N(^{13}CH$_3$)Mes]ZrCl$_2$ (7b). The ^{13}C-labeled analogue of **7a** was prepared in a manner similar to that for **7a** starting with **6b**. ^{1}H NMR data are analogous to data for **7a** except the resonance of the labeled methyl in the ^{1}H NMR appears as a doublet at 2.61 ppm ($^1J_{CH}$ = 134 Hz). The resonance of the labeled methyl appears as a singlet at 41.49 ppm in the ^{13}C{^{1}H} NMR spectrum.

[(MesNCH$_2$CH$_2$)$_2$NCH$_2$CH$_2$N(Me)Mes]ZrMe$_2$ (8a). A 1.0 M solution of MeMgI in ether (0.23 mL, 0.68 mmol) was added via syringe to a vigorously stirred suspension of **7a** (200 mg, 0.30 mmol) in ether (12 mL) at room temperature, and the reaction mixture was stirred for 1.5 h. Volatile solvents were removed under reduced pressure, and the residue was redissolved in toluene (∼8 mL). Excess dioxane was added to assist the removal of Mg salts. The mixture was stirred for 10 min to afford a milky slurry. Filtration through Celite, evaporation of the solvents from the filtrate, and trituration of the residue with pentane afforded **8a** as white crystalline material (160 mg, 0.24 mmol) in 80% yield: ^{1}H NMR δ 6.98 (s, 2, Ar), 6.93 (s, 2, Ar), 6.76 (s, 2, Ar), 3.67 (m, 2, CH$_2$), 3.03 (m, 2 + 4, CH$_2$), 2.62 (s, 3, NMe), 2.60 (m, 4, CH$_2$), 2.45 (s, 6, Me$_{Ar}$), 2.42 (s, 6, Me$_{Ar}$), 2.24 (s, 6, Me$_{Ar}$), 2.18 (s, 6, Me$_{Ar}$), 2.14 (s, 3, Me$_{Ar}$), 0.57 (s, 3, ZrMe), 0.25 (s, 3, ZrMe); ^{13}C{^{1}H} NMR δ 146.25, 145.30, 137.55, 136.57, 136.24, 135.84, 134.31, 130.64, 130.34, 130.10, 56.23 (CH$_2$), 55.85 (CH$_2$), 48.17 (CH$_2$), 43.57 (s, ZrMe), 43.09 (CH$_2$), 41.83 (NMe), 40.65 (s, ZrMe), 21.42 (Me$_{Ar}$), 21.16 (Me$_{Ar}$), 19.61 (Me$_{Ar}$), 19.19 (Me$_{Ar}$), 19.12 (Me$_{Ar}$).

[(MesNCH$_2$CH$_2$)$_2$NCH$_2$CH$_2$N(^{13}CH$_3$)Mes]ZrMe$_2$ (8b). The preparation of **8b** was analogous to that of **8a** starting with **7b**. NMR spectroscopy data are analogous to those in **8a** except

that the resonance of the labeled methyl in the ^{1}H NMR spectrum appears as a doublet at 2.62 ppm ($^1J_{CH}$ = 134 Hz).

[(MesNCH$_2$CH$_2$)$_2$NCH$_2$CH$_2$N(Me)Mes]Zr(^{13}CH$_3$)$_2$ (8c). Compound **8c** was prepared in a manner similar to that employed to prepare **8a** using ^{13}CH$_3$I as the alkylating agent. NMR data are analogous to data for **8a** except the resonances of the labeled methyls on Zr appear as doublets at 0.57 ppm ($^1J_{CH}$ = 114 Hz) and 0.25 ppm ($^1J_{CH}$ = 114 Hz).

{**[activ-MesNNMeMes]Zr**}**[B(C$_6$F$_5$)$_4$] (9a).** Compound **8a** (15 mg, 23 μmol) was dissolved in C_6H_5Br (1 mL), and the solution was left in a freezer for 10 min. A chilled solution of [Ph$_3$C][B(C$_6$F$_5$)$_4$] (21 mg, 23 μmol) in C_6H_5Br (~1 mL) was then added to the chilled solution of **8a**. The reaction mixture was allowed to warm to room temperature and was left at this temperature for 20 min. Addition of cold pentane (3 mL) precipitated a dark yellow solid, which was collected, dried, and redissolved in C_6D_5Br: ^{1}H NMR (C_6D_5Br, 20 °C) δ 6.83 (s, 2, Ar), 6.61 (s, 2, Ar), 6.41 (s, 1, Ar), 5.88 (s, 1, Ar), 4.04 (m, 2, CH$_2$), 3.67 (m, 1, CH$_2$), 3.52 (m, 1, CH$_2$), 3.45 (m, 1, CH$_2$), 3.31 (m, 1, CH$_2$), 3.12 (m, 2, CH$_2$), 3.03 (m, 1, CH$_2$), 2.84 (m, 1, CH$_2$), 2.78 (m, 1, CH$_2$), 2.55 (m, 1, CH$_2$), 2.51 (s, 3, NMe), 2.21 (s, 6, Me$_{Ar}$), 2.17 (s, 3, Me$_{Ar}$), 2.13 (s, 3, Me$_{Ar}$), 2.09 (s, 3, Me$_{Ar}$), 1.93 (s, 3, Me$_{Ar}$), 1.63 (b, 6, Me$_{Ar}$), 1.43 (AB, $^2J_{HH}$ = 14 Hz, 2, ZrCH$_2$).

{**[activ-MesNN^{13}MeMes]Zr**}**[B(C$_6$F$_5$)$_4$] (9b).** Compound **9b** was prepared from **8b** following the procedure employed for **9a**: ^{1}H NMR (C_6D_5Br, 20 °C) δ 6.83 (s, 2, Ar), 6.61 (s, 2, Ar), 6.41 (s, 1, Ar), 5.88 (s, 1, Ar), 4.04 (m, 2, CH$_2$), 3.67 (m, 1, CH$_2$), 3.52 (m, 1, CH$_2$), 3.45 (m, 1, CH$_2$), 3.31 (m, 1, CH$_2$), 3.12 (m, 2, CH$_2$), 3.03 (m, 1, CH$_2$), 2.84 (m, 1, CH$_2$), 2.78 (m, 1, CH$_2$), 2.55 (m, 1, CH$_2$), 2.51 (d, $^1J_{C-H}$ = 134 Hz, 3, N(^{13}CH$_3$)), 2.21 (s, 6, Me$_{Ar}$), 2.17 (s, 3, Me$_{Ar}$), 2.13 (s, 3, Me$_{Ar}$), 2.09 (s, 3, Me$_{Ar}$), 1.93 (s, 3, Me$_{Ar}$), 1.63 (b, 6, Me$_{Ar}$), 1.43 (AB, $^2J_{HH}$ = 14 Hz, 2, ZrCH$_2$); ^{1}H NMR (C_6D_5Br, 90 °C) δ 6.78 (s, 2, Ar), 6.61 (s, 2, Ar), 6.38 (s, 1, Ar), 5.87 (s, 1, Ar), 4.02 (m, 2, CH$_2$), 3.58 (m, 1, CH$_2$), 3.45 (m, 1, CH$_2$), 3.37 (m, 1, CH$_2$), 3.19 (m, 1, CH$_2$), 3.05 (m, 2, CH$_2$), 2.91 (m, 1, CH$_2$), 2.73 (m, 1, CH$_2$), 2.65 (m, 1, CH$_2$), 2.45 (m, 1, CH$_2$), 2.38 (d, $^1J_{CH}$ = 140 Hz, 3, N(^{13}CH$_3$)), 2.19 (s, 6, Me$_{Ar}$), 2.17 (s, 3, Me$_{Ar}$), 2.15 (s, 3, Me$_{Ar}$), 2.06 (s, 3, Me$_{Ar}$), 1.96 (s, 3, Me$_{Ar}$), 1.92 (b, 3, Me$_{Ar}$), 1.36 (m, 2, ZrCH$_2$), 1.27 (b, 3, Me$_{Ar}$).

{**[activ-MesNNMeMes]Zr**}**[BPh$_4$] (9a′).** Compound **8a** (120 mg, 180 μmol) was dissolved in toluene (~5 mL) at room temperature, and [(η^5-C$_5$H$_4$Me)$_2$Fe][BPh$_4$] (96 mg, 180 μmol) was added as a solid at room temperature to this colorless solution. The turquoise blue suspension slowly turned green and was stirred overnight at room temperature to afford a yellow slurry. A pale yellow solid was isolated by filtration on a frit, washed with pentane (3 × 1 mL), and dried under vacuum: ^{1}H NMR (C_6D_5Br) δ 7.88 (m, 8, *o*-H-BPh$_4$), 7.24 (m, 8, *m*-H-BPh$_4$), 7.08 (m, 4, *p*-H-BPh$_4$), 6.76 (s, 2, Ar), 6.59 (s, 2, Ar), 6.37 (s, 1, Ar), 5.87 (s, 1, Ar), 3.57 (m, 2, CH$_2$), 3.30−2.30 (mm, 10, CH$_2$), 2.26 (s, 3, NMe), 2.18 (s, 9, Me$_{Ar}$), 2.15 (s, 3, Me$_{Ar}$), 2.04 (s, 3, Me$_{Ar}$), 1.96 (s, 3, Me$_{Ar}$), 1.90 (b, 3, Me$_{Ar}$), 1.32 (m, 2, ZrCH$_2$), 1.30 (b, 3, Me$_{Ar}$). Anal. Calcd for $C_{58}H_{67}N_4Zr$: C, 75.64; H, 7.32; N, 6.08. Found: C, 75.41; H, 7.28; N, 5.96.

Kinetics of Decomposition of {[MesNMe]ZrMe}[B(C$_6$F$_5$)$_4$]. A cold solution (−30 °C) of [Ph$_3$C][B(C$_6$F$_5$)$_4$] (17.6 mg, 19.0 μmol) in C_6D_5Br (250 μL) was added to a cold solution (−30 °C) of [MesNMe]ZrMe$_2$ (9.0 mg, 19.0 μmol) in C_6D_5Br (250 μL) to give a 38.0 mM solution of {[MesNMe]ZrMe}[B(C$_6$F$_5$)$_4$], which was then transferred to a vial containing Ph$_2$CH$_2$ (3.2 mg), used as an internal standard, and finally to an NMR tube. The decomposition was followed by ^{1}H NMR at 20 and 60 °C using the methylene resonances of Ph$_2$CH$_2$ as the integration standard. A 19.0 mM solution of {[MesNMe]ZrMe}[B(C$_6$F$_5$)$_4$] in C_6D_5Br containing Ph$_2$CH$_2$ was prepared in a similar manner, and the decomposition kinetics were followed at 20 °C.

Kinetics of 1-Hexene Polymerization Initiated by {[MesNMe]ZrMe(PhNMe$_2$)}[B(C$_6$F$_5$)$_4$] (0.25 mM). A 12.6 mM stock solution of {[MesNMe]-ZrMe(PhNMe$_2$)}[B(C$_6$F$_5$)$_4$] in C_6D_5Br was prepared by adding [PhNHMe$_2$][B(C$_6$F$_5$)$_4$] (10.2 mg, 12.6 μmol) as a solid to a solution of [MesNMe]ZrMe$_2$ (6.0 mg, 12.6 μmol) in C_6D_5Br (1.0 mL). A stock solution of C_6Me_6 was prepared by dissolving C_6Me_6 (2.0 mg) in C_6D_5Br (1.0 mL). The {[MesNMe]ZrMe(PhNMe$_2$)}[B(C$_6$F$_5$)$_4$] stock solution (20.0 μL) and the C_6Me_6 stock solution (50 μL) were mixed in C_6D_5Br (920 μL), and the solution was cooled in the freezer (−30 °C) for 20 min. 1-Hexene (10 μL, 150 equiv) was then added while stirring the solution vigorously, and the consumption of olefin was monitored at 0 °C by ^{1}H NMR spectroscopy using C_6Me_6 as a standard.

Decomposition of the Polymerization Intermediates. A solution of [Ph$_3$C][B(C$_6$F$_5$)$_4$] (11.7 mg, 12.6 μmol) in C_6H_5Br (300 μL) was added to a solution of [MesNMe]ZrMe$_2$ (6.0 mg, 12.6 μmol) in C_6H_5Br (300 μL) to give a solution of {[MesNMe]-ZrMe}[B(C$_6$F$_5$)$_4$], which was cooled in the freezer (−30 °C) for 15 min. 1-Hexene (50 μL, 20 equiv) was added while the reaction was stirred vigorously. The reaction mixture was allowed to sit at room temperature for 2 days to give dark orange needles of **4^2**, according to X-ray diffraction analysis (unit cell determination).

X-ray Crystallography.[44] All specimens were handled similarly. Crystals were isolated from the mother liquor using a pipet to deposit a small quantity onto a microscope slide. These were then covered with deoxygenated heavy mineral oil (Exxon Paratone N) and manipulated, evaluated, and selected under a microscope. Specimens were mounted on a thin glass fiber with the aid of a mixture of Paratone oil and high-vac silicon grease using a rolled-up Kimwipe and transferred immediately to the cold stream (−90 °C) of the SMART CCD area detector diffractometer. (Graphite-monochromated Mo Kα radiation was provided by a sealed X-ray tube at 50 kV and 40 mA.) Unit cell parameters were determined using an automatic routine in SMART and refined prior to data collection.

Data were collected over a full hemisphere (1270 10 s frame images using a scan width of 0.3°, unless specified otherwise). These frames were then subjected to scanning for reflections and integration of data by the SAINT program to obtain a set of integrated reflection intensities. The resultant data were processed using the SHELXTL-Plus suite of programs. Direct methods were employed. Full-matrix least-squares (FMLS) refinements were computed on F^2 values with residuals calculated according to preset formulas. Hydrogen atoms were placed in idealized positions and refined using a riding model. The thermal parameters of the hydrogen atoms were set to 1.3 times one-third of the trace of the orthogonalized *U*-tensor of the carbon to which they are attached. Semiempirical absorption corrections were applied.

The enantiomeric form of **2b** was chosen on the basis of the Flack parameter.

Acknowledgment. R.R.S. thanks the Department of Energy (DE-FG02-86ER13564) for supporting this research.

Supporting Information Available: Fully labeled ORTEP drawings, atomic coordinates, bond lengths and angles, and anisotropic displacement parameters for **2b** and **3** are available free of charge via the Internet at http://pubs.acs.org. The Supporting Information for **4^2** was provided in a previous communication.[8]

OM010247K

(44) (a) *Bruker SMART V4.031 program for Bruker CCD X-ray diffractometer control*; Bruker Analytical X-ray Systems Inc.: Madison, WI, 1994. (b) *Bruker SAINT V4.028 program for reduction of data collected on Bruker CCD Area detector diffractometers*; Integration Software; Bruker Analytical X-ray Systems Inc.: Madison, WI, 1994−96. (c) Sheldrick, G. M. *SHELXTL Program Package*, Release 5.03; Bruker Analytical X-ray Systems Inc.: Madison, WI, 1995.